Nuclear Physics A535 (1991) 331–376
North-Holland

NUCLEAR
PHYSICS A

A GENERALIZED EQUATION OF STATE FOR HOT, DENSE MATTER

James M. LATTIMER

Department of Earth and Space Sciences, State University of New York at Stony Brook, Stony Brook, NY 11794, USA

F. DOUGLAS SWESTY

Department of Physics, State University of New York at Stony Brook, Stony Brook, NY 11794, USA

Received 6 June 1991

Abstract: An equation of state for hot, dense matter is presented in a form that is sufficiently rapid to use directly in hydrodynamical simulations, for example, in stellar collapse calculations. It contains an adjustable nuclear force that accurately models both potential and mean-field interactions, and it allows for the input of various nuclear parameters, some of which are not yet experimentally well-determined. These include the bulk incompressibility parameter, the bulk and surface symmetry energies, the symmetric matter surface tension, and the nucleon effective masses. This permits parametric studies of the equation of state in astrophysical situations. The equation of state is modelled after the Lattimer, Lamb, Pethick and Ravenhall LLPR compressible liquid-drop model for nuclei, and includes the effects of interactions and degeneracy of the nucleons outside nuclei. Account is also taken of nuclear deformations and the phase transitions from nuclei to uniform nuclear matter at subnuclear densities. Comparisons of this equation of state are made to the results of the LLPR model and the Cooperstein–Baron equation of state. The effects of varying the bulk incompressibility are also investigated.

1. Introduction

Under the conditions of interest in the study of supernovae and neutron stars, matter below nuclear densities is a mixture of nuclei, nucleons, leptons and photons. The leptons and photons interact rather weakly and may be treated as ideal Fermi and Bose gases, respectively. The main problem is to establish the state of the baryons. At low densities and temperatures and provided the matter does not have a large neutron excess, the baryons are bound in nuclei that are stable in the laboratory, and experimental information about the properties of nuclei may be directly employed. A Saha equation may be used to determine abundances for matter that is in "nuclear statistical equilibrium". For a larger neutron excess, properties of the relevant nuclei can be extrapolated from laboratory nuclei using the nuclear mass formula [cf. El Eid and Hillebrandt [1]) and Mazurek *et al.* [2])]. Under extreme conditions, however, this extrapolation breaks down. At higher densities, temperatures, or neutron excesses, the density of nucleons outside nuclei can be large, and a consistent treatment of both nuclei and nucleons, including modifications to the nuclear surface, is then desired. In addition, at finite temperature, nuclear excited states become populated and must be considered. Below the critical

0375-9474/91/$03.50 © 1991 - Elsevier Science Publishers B.V. All rights reserved

temperature of nuclear matter, above which nuclei are unstable, consideration must be paid to the phase equilibrium of the nuclear and nucleonic phases. Finally, in dense matter the space between nuclei becomes comparable to the nuclear size which leads to substantial modification of the nuclear Coulomb energy.

These effects have been consistently incorporated into nuclear models in three different techniques. Full Hartree-Fock calculations of unit cells of matter containing one nucleus have been calculated by Negele and Vautherin [3]) (at zero temperature) and Bonche and Vautherin [4]) and Wolff [5]) (at finite temperatures). Full Thomas-Fermi calculations, in which simplifying approximations to the nuclear wave function are incorporated, have been performed by Buchler *et al.* [6]) by Ogasawara and Sato [7]) and by Suraud [8]). Finally, unit-cell calculations using the finite temperature compressible liquid-drop model for the nucleus have been computed by Lattimer *et al.* [9]) (hereafter referred to as LLPR). The latter approach, while approximating that which is treated more exactly by the former approaches, has the virtues that its results are in close agreement with these other approaches, that it can be formulated as series of equilibrium conditions whose physical nature is readily apparent, and that it is significantly faster to compute. Nevertheless, it has been impractical, to date, to use even this approach directly in hydrodynamical simulations of supernovae, neutron-star births and neutron-star decompressions.

To make an equation of state (EOS) practical, one has two alternatives: construct a three-dimensional table of the relevant thermodynamic quantities as a function of the inputs (ρ, T, Y_e; ρ, e, Y_e; e, s, Y_e; or P, s, Y_e), or force further simplification in the equilibrium conditions of a liquid-drop approach in order to speed up their solution. The former task has, in fact, been carried out by Wolff [5]) with the full Hartree-Fock method, and by Lattimer [10]) with the LLPR model. Some numerical calculations have been performed using such tables [e.g., see the work of van Riper [11])]. However, the wide range of physical conditions, especially densities, encountered require such a table to be quite large in order to be both accurate and thermodynamically consistent. The extensive memory requirements for such a table thus render this approach impractical.

The latter approach has been considered in detail by Cooperstein and Baron [12,13]) and by Lattimer and coworkers [14]), and both models have been extensively used in hydrodynamical modeling. However, the existing models do not include some of the aspects of the LLPR model that we consider to be important. In particular, the degeneracy and interactions of the nucleonic phase below nuclear densities have been ignored, which may affect the phase transition to bulk matter and the properties of matter through the nuclear dissociation region at high densities and temperatures. The approach used in ref. [14]) also neglects the nuclear compression. In the Cooperstein-Baron model [12,13]), hereafter referred to as CB, the nuclear bulk and surface thermal energies have been combined into an "effective mass' term, so that the density and size dependencies of the nuclear specific heat are comprised, and, in

addition, the temperature dependence of the nuclear size has been neglected. Furthermore, the CB approach cannot be used for small proton concentrations as are encountered in very neutronized matter. In this paper, we wish to pursue an alternative approach to the earlier works, extending the model of ref. [14]), which is more directly coupled to the LLPR EOS.

An important modification to the earlier work that we wish to incorporate is the ability to input such nuclear parameters as the bulk incompressibility parameter, the saturation density, the surface energy, the nucleon effective mass and the bulk and surface components of the nuclear symmetry energy and the nuclear level density (i.e., the specific heat). Although some experimental information is available concerning each of these parameters, surprisingly large uncertainties currently exist concerning some of their values. In the previously mentioned equation of state calculations, one could alter these parameters, but it is then necessary to construct an entirely new table. However, if a sufficiently rigorous and rapid, but thermodynamically consistent, approximation to the basic equilibrium equations existed, studies could be carried out without the need to construct tables and simulations with different sets of nuclear parameters could be directly performed. A first step was taken with the CB EOS by Baron *et al.* [48]), by Bruenn [15]) and by Myra and Bludman [16]), who examined the results of variations in the bulk symmetry coefficient. However, the variations considered were inconsistent with nuclear mass systematics.

Our approach in this paper is to follow the detailed calculations of LLPR, further simplifying the free energy function of the finite temperature compressible liquid-drop model and thus the equilibrium equations derived from its minimization. We seek a form in which a lower order Newton-Raphson iteration is achieved (the original LLPR model is 5-dimensional) and to ensure that the results follow those of LLPR to a reasonable accuracy, for the same underlying nuclear force. However, our model will contain the nuclear parameters previously mentioned as inputs which can be easily, and consistently, altered. It will also be straightforward to substitute any other model for the nucleon–nucleon force provided that an expression for the energy as a function of density, temperature and composition is available. In as much as the model presented here is able to reproduce the original LLPR calculations, we have confidence that the detailed results for other choices of nuclear parameters or forces will also be faithfully represented. Our goal is to present our calculations as an algorithm that is sufficiently rapid and flexible to be useful in many astrophysical calculations.

In sect. 2, the model for the free energy is discussed, and the equilibrium conditions are derived in sect. 3. Sect. 4 details the solution of these conditions and the evaluation of all the relevant thermodynamic quantities. In sect. 5 we make a detailed comparison of our results with those of the models of LLPR and CB. Our conclusions are offered in sect. 6.

2. The model

2.1. GENERAL CONSIDERATIONS

In the range of temperatures and densities that we are considering in this paper, matter may be modeled as a mixture of electrons, positrons, photons, free neutrons, free protons, alpha particles, and a single species of heavy nuclei. The alpha particles represent the distribution of light nuclei that are actually present, while the single heavy nucleus represents the average of an ensemble of heavy nuclei. The accuracy of the latter approximation has been considered previously [17]), where it was shown that thermodymamic quantities in the single-nucleus approximation differ from those in the general case by at most a negligibly small amount. The electrons are treated as non-interacting ultrarelativistic particles in pair equilibrium, and, as was discussed in LLPR, electron-screening effects may be ignored because the electron-screening length is larger than the separation of the ions. Inclusion of neutrinos and muons and the effects of the rest mass of the electrons, all of which we will neglect, may be easily performed because the thermodymamics of the leptons is largely independent of that of the baryons. Although we will model the EOS to arbitrarily high densities, our interest is mostly in the region below about twice nuclear density. It is therefore not necessary for us to consider, at present, possible additional physics such as pion or kaon condensation, hyperons, and the quark-hadron phase transition.

In this model we assume that the different forms of matter are in equilibrium with respect to strong and electromagnetic interactions. We do not assume the condition of β-equilibrium, since equilibrium with respect to weak interactions is often not achieved within the timescales of many astrophysical phenomena.

The heavy nuclei, at densities well below nuclear density, are treated as being in a b.c.c. lattice which maximizes the separation of the ions. In accordance with the Wigner–Seitz approximation each heavy ion is considered to be surrounded by a charge-neutral spherical cell consisting of a less dense vapor of neutrons, protons and alpha particles as well as electrons. The volume of this cell is given by $V_c = n_N^{-1}$, where n_N is the number density of heavy nuclei.

The balance of matter between the various phases is given by the distribution that is most thermodynamically favorable for a given baryon number density n, temperature T and proton fraction Y_e. For a single representative heavy nucleus, the seven free variables of the model governing this distribution are the number densities of heavy nuclei (n_N) and alpha particles (n_α), the number density and proton fraction of nucleons outside nuclei (n_o and x_o, respectively), the nuclear radius (r_N), and the nucleon density and proton fraction inside nuclei (n_i and x_i, respectively). The additional variable considered by LLPR, the number of neutrons in the neutron skin of the nucleus, is not relevant here because we are ignoring the presence of the neutron skin. The consequences of this are discussed in sect. 5. The optimization is subject to the joint constraints of conservation of baryon number

and electric charge. Thus the model has five independent internal variables. The most thermodynamically favorable state will be the one that minimizes the Helmholtz free-energy density with respect to these variables. The minimization, done by taking partial derivatives of the free energy with respect to these five variables, yields a system five equilibrium equations which can then be solved for the equilibrium values of the variables.

We adopt the convention of measuring all baryon energies with respect to the neutron rest mass, in accord with LLPR. All Coulomb energies are included with the nuclear free energy. Also, all temperatures and energies are quoted in units of MeV, all energy densities and pressures are in units of MeV $\cdot$ fm^{-3}, and entropies are measured in units of Boltzmann's constant.

The Helmholtz free-energy density can be written as the sum of the free-energy densities of the individual constituents of the matter. Thus

$$F = F_o + F_\alpha + F_N + F_e + F_\gamma, \tag{2.1}$$

where F_o, F_α, F_N, F_e and F_γ are the free-energy densities of nucleons outside nuclei, alpha particles, heavy nuclei, electron-positron pairs and photons, respectively. As mentioned previously, F_e and F_γ are independent of the baryons, and will play no role in the equilibrium equations.

In order to arrive at a set of equilibrium equations that can be solved via a Newton-Raphson iteration scheme, it is necessary to specify the free-energy densities. In general, one can reduce the dimensionality of the computational algorithm, and increase the speed, by introducing approximations in the free energies. It is hoped that sufficiently clever approximations can lead to arbitrary close agreement to the more exact solution represented by the results of LLPR. If simplifications are made in the equilibrium conditions instead, thermodynamic consistency is jeopardized, since thermodynamic equilibrium demands that the free energy must be minimized *exactly*. In particular, if the free energy is not minimized exactly, the pressure, entropy and "muhat", given by

$$\begin{aligned} P &= n^2 \partial(F/n)/\partial n|_{T,Y_e}, \\ s &= -\partial(F/n)/\partial T|_{n,Y_e}, \\ \hat{\mu} - \mu_e \equiv \mu_n - \mu_p - \mu_e &= -\partial(F/n)/\partial Y_e|_{n,T}, \end{aligned} \tag{2.2}$$

will be inconsistent. In this case the first law of thermodynamics will no longer be satisfied, and an artificial buildup of entropy in numerical simulations will occur. Nevertheless, if the free-energy function is simplified too much, in an attempt to find simple equilibrium equations, the resulting EOS may not be very realistic. A final consideration that influences the scheme will use is its overall speed, which is dictated by the number of equilibrium equations and the quality of iterative convergence. The algorithms presented in this paper, while representing some compromises in the interest of computational speed, do not sacrifice any essential physics of which we are aware.

In a portion of the region of the density-temperature plane in which we are interested, the differences from LLPR are miniscule since the electron, bulk nuclear, and/or photon contributions dominate the free energy. These contributions are treated in our model in essentially the same fashion as they were treated by LLPR. The largest differences in the two approaches generally occur in the nuclear dissociation region in which the various baryon abundances undergo rapid changes.

As has been known since the pioneering studies of neutron-star matter [18]), a phase transition occurs at about one-half the nuclear density ($n_s \simeq 0.16$ fm^{-3}) between the phase with nuclei and a uniform bulk nuclear matter phase. This phase transition was found to be first order, since it is accompanied by a small energy change. Later studies [19,20]) have indicated that this abrupt transition may be smoothed by a series of smaller transitions (to bubbles, spaghetti, lasagna, etc.), which would have the effect of further softening the EOS in this region. Nevertheless, a significant phase transition from a distorted nuclear (or inside-out bubble) phase to the uniform bulk phase remains. The adiabatic index of the matter is very sensitive to how this transition from nuclei to bulk matter is taken into account, and, given the importance of the adiabatic index in hydrodynamical calculations, we will treat this transition as exactly as possible. This is done by modifying the Coulomb and surface energies of the nuclei to include distortions in the nuclear shape and the appearance of bubbles, and by including an explicit Maxwell construction between the nuclei phase and the bulk nuclear matter phase at fixed temperature and Y_e. The limiting densities and temperatures of the two phases, i.e., the phase boundaries, are computed during the initial call to the equation of state and stored in tabular form. We emphasize that an alternative approach of artifically smoothing thermodynamic quantities across the phase transition is incorrect, and misrepresents the pressure and the adiabatic index in the transition region.

2.2. NUCLEAR PARAMETERS

There are a number of nuclear parameters that the equation of state will include. All of them, in principle, can be experimentally determined, but, in practice, some of them have relatively large uncertainties. They may, alternatively, be calculated from a given nuclear force by modeling heavy nuclei. Since matter in laboratory nuclei is cold ($T \simeq 0$), nearly symmetric ($x_i = Z/A \simeq \frac{1}{2}$), and close to the saturation density ($n_s \simeq 0.16$ fm^{-3}), it is customary to write the following expansion for the free energy per baryon, $f_{\rm bulk}$, of bulk nuclear matter:

$$f_{\rm bulk}(n, x, T) \simeq -B - \Delta x + \tfrac{1}{18} K_s (1 - n/n_s)^2 + S_v (1-2x)^2 - a_v T^2 + \cdots . \quad (2.3)$$

Here, Δ is the neutron-proton mass difference, 1.293 MeV, and must be included because our energy is measured with respect to the neutron rest mass. We can identify the following parameters:

(i) n_s - The saturation density of symmetric nuclear matter. Values in the range 0.145-0.17 fm^{-3} are commonly assumed. We will employ in our standard calculation the Skyrme I' force value of $n_s = 0.155$ fm^{-3}.

(ii) $B = -f_{\rm bulk}(n_s, \frac{1}{2}, 0) - \frac{1}{2}\Delta$ - The binding energy of saturated, symmetric nuclear matter. Values for B, derived from nuclear mass formula fits [21,22]), lie in the range 15.85-16.2 MeV. We will employ in our standard calculation the Skyrme I' force value of $B = 16.0$ MeV.

(iii) $K_s = \frac{1}{9}n_s^2(\partial^2 f_{\rm bulk}/\partial n^2)|_{n_s,1/2,0}$ - The incompressibility of bulk nuclear matter. Estimates in the literature are in the range 150-300 MeV [refs. [23-26])]. The Skyrme I' force [27]) used by LLPR has $K_s = 375$ MeV, and for comparison purposes we have employed this value in this paper in spite of the fact that it seems unrealistically high. However, we present results from the more realistic values $K_s = 220$ and 180 MeV in sect. 6.

(iv) $S_v = \frac{1}{8}(\partial^2 f_{\rm bulk}/\partial x^2)|_{n_s,1/2,0}$ - The symmetry energy parameter of bulk nuclear matter. Estimates have been derived from mass formulae [21,28,29,22]) and from the energy of the giant dipole resonance [30]) and range from 27.5 to 36.8 MeV. We will employ in our standard calculation the Skyrme I' force value of $S_v = 29.3$ MeV.

(v) $a_v = -\frac{1}{2}(\partial^2 f_{\rm bulk}/\partial^2 T)|_{n_s,1/2,0}$ - The bulk level density parameter. Using the fact that nucleons are nearly degenerate, nonrelativistic fermions, it is given by

$$a_v = \frac{2m^*}{\hbar^2}\left(\frac{\pi}{12 n_s}\right)^{2/3} \simeq \tfrac{1}{15} m^*/m \ \text{MeV}^{-1}, \tag{2.4}$$

where m^* is the nucleon effective mass for saturated, symmetric matter. Determination of nuclear-energy levels from Hartree-Fock calculations [31]) and the position of the giant dipole resonance [30]) imply that m^* is somewhat less than the bare nucleon mass m, $m^*/m \sim 0.7$-0.9. However, nuclear-mass fits [32]), fission-barrier fits [33]) and the reproduction of the density of single-particle energies near the Fermi surface [34]) argue instead that $m^*/m \sim 1$-1.2. Although the force Skyrme I' has $m^*/m \simeq 0.9$, we will take $m^*/m = 1$ because of computational simplicity. This has very little effect on the comparison between our results and those of LLPR.

In its simplest form, the liquid-drop model for an isolated nucleus may be written

$$f_N = f_{\rm bulk} + f_s + f_C, \tag{2.5}$$

where the surface energy per baryon is $f_s(n_i, x_i, T) = (4\pi r_N^2/A)\sigma(x_i, T)$ and the Coulomb energy per baryon is $f_C(n_i, x_i) = 3Z^2e^2/(5r_N A)$, where $A = \frac{4}{3}\pi n_i r_N^3$. The Coulomb energy is independent of T. The surface tension σ may be expanded in a fashion analogous to the bulk energy:

$$f_s A = 4\pi r_N^2 \sigma(x_i, T) \simeq 4\pi r_N^2 \sigma(\tfrac{1}{2}, 0) - A^{2/3}[S_s(1-2x_i)^2 + a_s T^2] + \cdots. \tag{2.6}$$

Note that there is no dependence of σ upon density (n_i) because the bulk nucleon fluid inside the nucleus is in equilibrium with that outside the nucleus (in this case, a vacuum). The equilibrium is only possible for one value of n_i for given values of x_i and T. Thus, the surface nuclear parameters are

(vi) $\sigma_s \equiv \sigma(\frac{1}{2}, 0)$ - The surface tension of symmetric nuclear matter. Values are again derived from nuclear-mass formula fits[21,28,29,22]) and values in the range 1.06–1.34 MeV · fm^{-3} have been obtained. We will employ in our standard calculation the Skyrme I' force value of $\sigma_s = 1.15$ MeV · fm^{-3}.

(vii) $S_s = -\frac{1}{8}A^{1/3}\partial^2 f_s/\partial x_i^2)|_{n_s,1/2,0}$ - The surface symmetry energy parameter. From the fitting of nuclear masses it is known that a strong correlation [35]) exists between values of S_s and S_v:

$$S_s \sim 40(\tfrac{1}{30}S_v \text{ MeV})^{6-9} \text{ MeV}. \tag{2.7}$$

Estimates from nuclear-mass formula fits [21,28,29,22]) lie in the range 18–180 MeV. We will employ in our standard calculation the Skyrme I' force value of $S_s = 45.8$ MeV.

(viii) $a_s = -\frac{1}{2}A^{1/3}(\partial^2 f_s/\partial T^2)|_{n_s,1/2,0}$ - The surface level density parameter. This is defined similarly to a_v and typical values lie in the range 0.05–0.2 MeV^{-1}.

To summarize, our equation of state requires specification of the above 8 parameters. However, fits to nuclear masses, and theory, constrain the realistic ranges of these parameters. (For example, as we discuss in sect. 2.6, a theoretical relationship may be found which connects the values of K_s, σ_s, and a_s.) In particular, the members of the pairs (B, σ_s), (S_v, S_s) and (K_s, a_s) cannot be treated independently: a choice of a value for one member restricts allowable values for the other. Thus, in practice, only 5 of these parameters can independently affect the equation of state. We now consider in turn the free-energy densities of each of the constituents of matter.

2.3. BULK ENERGY OF NUCLEONS

One aspect of LLPR that is essential to a consistent treatment of both nucleons and nuclei is to determine the bulk portions of their free energies from the same function of density and temperature. Whereas LLPR used for this function a standard momentum-dependent Skyrme-type parameterization [27]) which treats nucleon–nucleon interactions as being local, we will employ a simpler momentum-dependent potential model. The parameters of this interaction hamiltonian will be determined by the properties of zero-temperature symmetric nuclear matter at its saturation density n_s, namely the binding energy E_s, the bulk symmetry energy S_v, and the bulk incompressibility parameter K_s. It reproduces the thermodynamic properties of bulk nuclear matter accurately for any Skyrme-type interaction. With a small modification [36]) to allow for finite-range effects, it can approximate forces with more complicated momentum dependences, such as those of Gale *et al.* [37]), Gogny [38]) and Welke *et al.* [39]), at least in the density regime below twice nuclear matter density. It should be emphasized that this or another nuclear force model may be easily substituted for the one we have chosen in this paper. The resulting algebra may become more complicated, but, in principle, the technique for calculating the EOS will be essentially unaltered. Much of the following treatment follows the work of Lattimer and Ravenhall [27]).

The bulk internal energy density of interacting nucleons at finite temperature will be approximated as

$$E_{\rm bulk}(n, x, T) = \sum_t \frac{\hbar^2 \tau_t}{2m_t^*} + [a + 4bx(1-x)]n^2 + cn^{1+\delta} - xn\Delta, \tag{2.8}$$

where the first term contains the non-relativistic fermion kinetic energies (t, the isospin, is n or p), the second term represents two-body interactions and the third term the influence of multibody interactions. Here, $x = n_{\rm p}/n$ and $n = n_{\rm n} + n_{\rm p}$ are the proton fraction of the matter and its total baryon density, respectively. The quantity m_t^* is a density-dependent effective nucleon mass, which incorporates the force's momentum dependence. It can be adequately represented in the same way as for Skyrme forces as

$$\hbar^2/2m_t^* = \hbar^2/2m + \alpha_1 n_t + \alpha_2 n_{-t}, \tag{2.9}$$

where α_1 and α_2 are constant parameters and $-t$ is the opposite isospin of t. The constants a, b, c and δ are parameters of the nuclear force, and will be determined (see below) from a given set of experimental inputs. Again, the last term in eq. (2.8) arises because we choose to write all energies relative to the neutron rest mass $m_{\rm n}$.

The entire temperature dependence of the nuclear force is implicitly included in the nucleon kinetic energy densities τ_t, which are

$$\tau_t = \frac{1}{2\pi^2}\left(\frac{2m_t^* T}{\hbar^2}\right)^{5/2} F_{3/2}(\eta_t). \tag{2.10}$$

In this expression, F_i is a Fermi integral:

$$F_i(\eta) = \int_0^\infty u^i [1 + \exp(u - \eta)]^{-1}\, {\rm d}u. \tag{2.11}$$

These integrals (and their inverses, see eq. (2.15) below) are solved by spline interpolation among values taken from the CERN subroutine library. To ensure thermodynamic consistency, accurate fits (to about 1 part in 10^4) are necessary. The degeneracy parameter η_t is related to the chemical potential μ_t and the force's potential V_t via

$$\eta_t = (\mu_t - V_t)/T, \tag{2.12}$$

where

$$V_t \equiv \left.\frac{\delta E_{\rm bulk}}{\delta n_t}\right|_{\tau_{\rm n}, \tau_{\rm p}, n_{-t}} = \alpha_1 \tau_t + \alpha_2 \tau_{-t} + 2an + 4bn_{-t} + c(1+\delta)n^\delta - \Delta\delta_{tp}. \tag{2.13}$$

Here, δ_{tp} is the Kronecker delta. The parameter η_t is itself related directly to the densities and temperature:

$$n_t = \frac{1}{2\pi^2}\left(\frac{2m_t^* T}{\hbar^2}\right)^{3/2} F_{1/2}(\eta_t). \tag{2.14}$$

Inversion of this relation yields

$$\eta_t = F_{1/2}^{-1}[2\pi^2 n_t (\hbar^2/2m_t^* T)^{3/2}], \tag{2.15}$$

which enables evaluation of thermodynamic quantities from knowledge of n_t and T. The entropy per baryon may be written [27])

$$s_{\rm bulk} = \sum_t \left(\frac{5\hbar^2 \tau_t}{6m_t^* T} - n_t \eta_t \right) \Big/ n , \tag{2.16}$$

and the bulk free energy per baryon is

$$f_{\rm bulk} = E_{\rm bulk}/n - T s_{\rm bulk} . \tag{2.17}$$

The pressure may be found from

$$\begin{aligned} P_{\rm bulk} &= n^2 (\partial f_{\rm bulk}/\partial n) = \sum_t n_t \mu_t - n f_{\rm bulk} \\ &= \sum_t (5\hbar^2/6m_t^* - \hbar^2/2m)\tau_t + [a + 4bx(1-x)]n^2 + c\delta n^{1+\delta} . \end{aligned} \tag{2.18}$$

The nuclear force parameters are evaluated by reference to laboratory nuclear matter, that is, zero-temperature, symmetric nuclear matter at its saturation density. In the case of $T=0$ and $x=0.5$, the bulk energy, pressure and incompressibility ($K = 9{\rm d}P/{\rm d}n$) become

$$\left.\begin{aligned} E_{\rm bulk}/n &= \alpha (n/n_{\rm s})^{2/3} + (a+b)n + cn^{\delta} - \tfrac{1}{2}\Delta , && \text{(2.19a)} \\ P_{\rm bulk}/n &= \tfrac{2}{3}\alpha (n/n_{\rm s})^{2/3} + (a+b)n + c\delta n^{\delta} , && \text{(2.19b)} \\ \tfrac{1}{9}K_{\rm bulk} &= \tfrac{10}{9}\alpha (n/n_{\rm s})^{2/3} + 2(a+b)n + c\delta(1+\delta)n^{\delta} . && \text{(2.19c)} \end{aligned}\right\} \quad T=0, \quad x=\tfrac{1}{2} .$$

Here $\alpha = (3\hbar^2/10m^*)(\frac{3}{2}\pi^2 n_{\rm s})^{2/3}$ and $m_{\rm n}^* = m_{\rm p}^* = m^*$ for symmetric matter. The symmetry energy is adequately represented for most interactions [36]) by the difference between the neutron matter energy ($E_{\rm bulk}|_{n_{\rm s},\, x=0,\, T=0}$) and the symmetric matter energy ($E_{\rm bulk}|_{n_{\rm s},\, x=1/2,\, T=0} + \frac{1}{2}\Delta \equiv -B$). Therefore, we have for the bulk symmetry parameter

$$S_{\rm v} \equiv \frac{1}{8n} \frac{\partial^2 E_{\rm bulk}}{\partial^2 x} \bigg|_{n_{\rm s},\, x=1/2,\, T=0} \simeq \alpha (2^{2/3} - 1) - b n_{\rm s} . \tag{2.20}$$

At the saturation density $n_{\rm s}$, the zero temperature, symmetric matter pressure vanishes. The parameters a, b, c and δ may now be determined from the experimental parameters $n_{\rm s}$, B, $K_{\rm s} \equiv K_{\rm bulk}|_{n_{\rm s},\, x=\frac{1}{2},\, T=0}$, m^* and $S_{\rm v}$:

$$\delta = \frac{K_{\rm s} + 2\alpha}{3\alpha + 9B} , \tag{2.21a}$$

$$b = [\alpha (2^{2/3} - 1) - S_{\rm v}]/n_{\rm s} , \tag{2.21b}$$

$$a = \frac{\delta[\alpha + B] - \frac{2}{3}\alpha}{n_{\rm s}(1-\delta)} - b , \tag{2.21c}$$

$$c = \frac{K_{\rm s} + 2\alpha}{9\delta(\delta - 1) n_{\rm s}^{\delta}} . \tag{2.21d}$$

For the purpose of choosing nuclear force parameters for the calculation described in this paper, we will assume, for simplicity, that $m^* = m$ and $\alpha_1 = \alpha_2 = 0$. We will,

however, keep the effective mass terms in the equations that follow, so that the generalization of this assumption can be seen. We emphasize that this assumption has little effect on the equation of state below nuclear matter density, since the change in the effective mass with overall density n is negligible. One should not confuse the effective mass with the effective density dependence of the specific heat contribution from the surface [12,13]), which is explicitly included in our formulation (see the next section). With the further choices $B = 16$ MeV, $n_s = 0.155$ fm^{-3}, $K_s = 375$ MeV and $S_v = 29.3$ MeV, which will match the Skyrme I' parameter set used by ref. [9]), we find $\delta = 2.002$, $a = -285.1$ MeV $\cdot$ fm^3, $b = -107.1$ MeV $\cdot$ fm^3 and $c = 968.0$ MeV $\cdot$ fm^6.

The multibody parameter δ is necessarily restricted to values greater than unity. Otherwise this term, rather than the two-body term and/or the kinetic energy term, will dominate the energy at low densities, which is unphysical. In general, since $K_s \gg 2\alpha$, eq. (2.21a) shows that δ is roughly proportional to K_s. For the values of B, n_s and S_v chosen above, the effective interaction given by eq. (2.8) is thus limited to a symmetric matter incompressibility parameter $K_s \geq 166$ MeV, assuming $\alpha_1 = \alpha_2 = 0$. Although this value seems to be well below recent experimental measurements, this restriction should be kept in mind. The inclusion of additional terms in eq. (2.8), such as the effects of finite-range forces, however, can remove this restriction.

2.4. NUCLEONS OUTSIDE NUCLEI AND ALPHA PARTICLES

Outside the heavy nuclei, there is a gas of nucleons and α-particles. We take into account interactions between this gas and the nuclei by excluding the gas from occupying the nuclear volume. Similarly, we take into account interactions between α-particles and the nucleon gas outside nuclei by treating the α-particles as hard spheres of effective volume $v_\alpha = 24$ fm^{-3}. These approximations and the magnitude of v_α are discussed in more detail in LLPR. We will see below, in sect. 3.1, that the inclusion of the α-particle excluded volume is not only physically reasonable, but also practically motivated.

Defining $u = V_N / V_c$ as the fraction of space occupied by nuclei, where V_N is the volume of a single nucleus, the fraction of space available to α-particles is just $1 - u$. The volume fraction occupied by α-particles is then $(1-u)n_\alpha v_\alpha$, where n_α is the number of α-particles per unit volume in the space outside nuclei. As a result, the volume fraction available to nucleons outside nuclei is

$$1 - u - (1-u)n_\alpha v_\alpha = (1-u)(1 - n_\alpha v_\alpha)\,. \tag{2.22}$$

The free-energy density of the outside nucleons, obtained from eq. (2.17), may be written as

$$F_o = (1-u)(1-n_\alpha v_\alpha) n_o f_{\rm bulk}(n_o, x_o, T) = (1-u)(1-n_\alpha v_\alpha) n_o f_o\,, \tag{2.23}$$

where $f_0 \equiv f_{\rm bulk}(n_{\rm o}, x_{\rm o}, T)$. The subscript o will generally refer to outside nucleons. We will find it more convenient to use $n_{\rm no}$ and $n_{\rm po}$, instead of $n_{\rm o}$ and $x_{\rm o}$ to refer to the outside nucleons.

The alpha particles are treated as non-interacting Boltzmann particles:

$$F_\alpha = (1-u) n_\alpha f_\alpha = (1-u) n_\alpha (\mu_\alpha - B_\alpha - T)\,, \tag{2.24}$$

where $B_\alpha = 28.3$ MeV is the binding energy of an alpha particle relative to free nucleons. The alpha chemical potential is

$$\mu_\alpha = T \ln (n_\alpha / 8 n_{\rm Q})\,. \tag{2.25}$$

We have used the abbreviation $n_{\rm Q} = (mT/2\pi\hbar^2)^{3/2}$. We also note that the alpha pressure is just $P_\alpha = n_\alpha T$.

2.5. HEAVY NUCLEI

The contribution to the free-energy density due to heavy nuclei consists of bulk, surface, Coulomb and translational contributions. Electrostatic contributions from the Wigner-Seitz approximation are included with the Coulomb contributions. We write the free-energy density as

$$\begin{aligned} f_{\rm N} &= {\rm F}_{{\rm bulk},i} + F_{\rm S} + F_{\rm C} + F_{\rm H} \\ &= A n_{\rm N} (f_{\rm bulk}(n_{\rm i}, x_{\rm i}, T) + f_{\rm s} + f_{\rm C} + f_{\rm H}) = u n_{\rm i} (f_{\rm i} + f_{\rm s} + f_{\rm C} + f_{\rm H}) \end{aligned} \tag{2.26}$$

where A is the baryon number of the average nucleus. Our notation is that upper case F's are free-energy densities and lower case f's are free energies per baryon. In the right-hand side of eq. (2.26) we have made the substitutions $f_{\rm i} \equiv f_{\rm bulk}(n_{\rm i}, x_{\rm i}, T)$ and $A = n_{\rm i} V_{\rm N}$, the subscript i referring to nucleons inside the nucleus. The nuclear radius is $r_{\rm N}$, defined by $V_{\rm N} \equiv \frac{4}{3}\pi r_{\rm N}^3$. Note that the bulk energies of the nucleons both inside and outside nuclei are calculated with the same energy expression. We now consider the finite-size (non-bulk) contributions to the free energy of heavy nuclei.

2.6. SURFACE ENERGY

The surface contributions are taken from LLPR with some modifications. The relevant calculation is to find the surface tension between two infinite slabs of nuclear matter: a dense phase representing nuclei, and a light phase representing the nucleon vapor. Because of the conditions of bulk equilibrium across the surface between the two fluids, the surface tension σ for a given temperature is a function of only one of the four variables $n_{\rm i}$, $x_{\rm i}$, $n_{\rm o}$ and $x_{\rm o}$. As in LLPR, we thus choose to parameterize σ in terms of $x_{\rm i}$ and T alone. Like LLPR, we have neglected the effects of curvature on the surface energy. In contrast to LLPR, we have chosen not to explicitly include the neutron skin of the surface in our model. To do so would

require the use of a higher-dimensioned Newton-Raphson iteration scheme. Thus, we parameterize the energy in terms of the *average* value of the proton fraction, $x_i = Z/A$, in the nucleus, rather than in terms of the *central* value of the proton fraction. Thus, as shown in LLPR and Kolehmainen *et al.*[40]) the surface thermodynamic potential in LLPR's calculation plays the role of the surface free energy here. The net result is that the total symmetry energy of a nucleus may be written as $A(1-2x_i)^2(S_v - S_s A^{-1/3})$, compared to the expression $A(1-2x_i)^2 S_v^2/(S_v + S_s A^{-1/3})$ which follows from an explicit treatment of the neutron skin. (We note that these two symmetry energy expressions are identical to the forms found in the nuclear liquid-*drop* model and the nuclear *droplet* model, respectively.) In the limit $A \to \infty$, these forms are equivalent. However, in the laboratory or presupernova star situations, in which $4 < A^{1/3} < 10$, differences are apparent. At least, some of the large spread in published determinations of values of S_s relative to S_v is due to this model dependence.

We have used the results of Thomas-Fermi surface calculations[41]) to determine the full x_i and T dependences of the surface free energy per unit area. We have found that, with slight modification, the functional form used by LLPR for the Skyrme I′ force is valid for general energy functionals of the form eq. (2.8). We use

$$\sigma(x_i, T) = \sigma_s h\left(\frac{T}{T_c(x_i)}\right) \frac{16+q}{x_i^{-3} + q + (1-x_i)^{-3}} \text{ MeV} \cdot \text{fm}^{-2}, \tag{2.27}$$

where the temperature dependence is taken to be

$$h\left(\frac{T}{T_c(x_i)}\right) = \begin{cases} [1-(T/T_c(x_i))^2]^2 & T \leq T_c(x_i)\,; \\ 0 & T > T_c(x_i)\,. \end{cases} \tag{2.28}$$

Note that $\sigma_s \equiv \sigma(0.5, 0)$. It is easily found that q is related to the surface symmetry coefficient by

$$q = 384\pi r_o^2 \sigma_s / S_s - 16\,, \tag{2.29}$$

where $r_o = r_N/A^{1/3} \simeq (3/4\pi n_s)^{1/3}$. $T_c(x_i)$ represents the maximum temperature, for a given x_i, for which the nuclear phase may coexist with the nucleon vapor. $T_{co} = T_c(\frac{1}{2})$ is the critical temperature of symmetric nuclear matter, which can be determined by the relations

$$\left.\frac{\partial P_{\text{bulk}}}{\partial n}\right|_{x=1/2} = \left.\frac{\partial^2 P_{\text{bulk}}}{\partial n^2}\right|_{x=1/2} = 0\,. \tag{2.30}$$

T_{co} is essentially determined[42]) by K_s, m^* and n_s, such that $T_{co} \propto \sqrt{K_s/m^*}\, n_s^{-1/3}$. We have found that Thomas-Fermi surface calculations are well approximated by the relation $T_c(x_i) = 4T_{co}x_i(1-x_i)$. Combining these results, we approximate $T_c(x_i)$ by

$$T_c(x_i) = 87.76\left(\frac{K_s}{375 \text{ MeV}}\right)^{1/2}\left(\frac{0.155 \text{ fm}^{-3}}{n_s}\right)^{1/3} x_i(1-x_i) \text{ MeV}\,. \tag{2.31}$$

The exact relation between T_{co} and K_s, and the approximation eq. (2.31), are shown in fig. 1 for the case $n_s = 0.16\ \mathrm{fm}^{-3}$ and $m^* = m$.

The particular form for $h(T/T_c)$ we use has the property that its temperature derivative vanishes at T_c. This ensures that surface contributions to the entropy disappear as $T \to T_c$. Although the T and x_i dependences of h are not the same as in LLPR, the differences are not important. Note that the surface contribution to the nuclear specific heat is

$$a_s = 8\pi r_0^2 \sigma_s / T_{co}^2 , \tag{2.32}$$

which, according to eq. (2.31), is proportional to $\sigma_s m^*/K_s$.

In summary, the free energy per baryon of the surface will be written as

$$f_s = \frac{4\pi r_N^2 \sigma(x_i, T)}{A} = \frac{3\sigma(x_i, T)}{r_N n_i} . \tag{2.33}$$

2.7. COULOMB ENERGY

The Coulomb contributions to the free energy of nuclei in the low-density, low-temperature limit may be derived using the Wigner-Seitz approximation [18]).

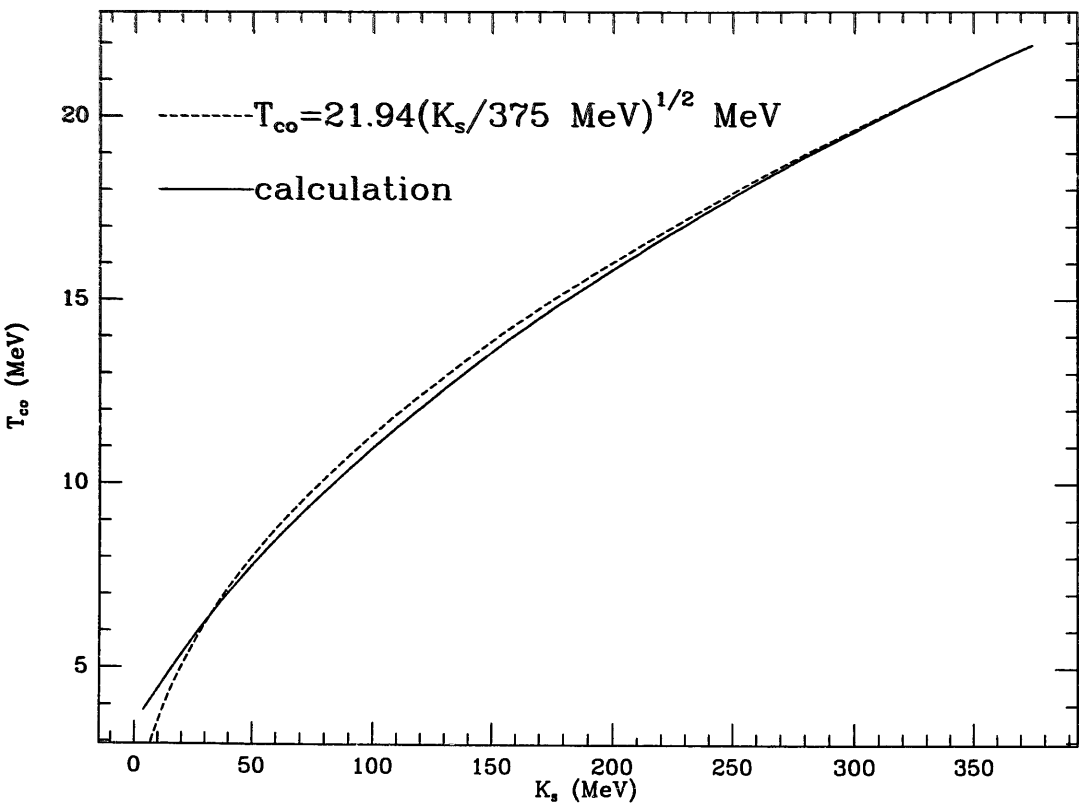

Fig. 1. T_{co} versus bulk incompressibility parameter, K_s.

This can be written as

$$f_C = \frac{3}{5A}\left(\frac{Z^2e^2}{r_N}\right) D(u) = \tfrac{4}{5}\pi e^2 x_i^2 r_N^2 n_i D(u)\,, \tag{2.34}$$

where e is the electron charge and $D(u) \equiv 1 - \frac{3}{2}u^{1/3} + \frac{1}{2}u$. In contrast to the treatment of LLPR, we have neglected screening effects of the vapor of protons and alpha particles, so the effective nuclear charge is just Z. This is justified except, perhaps, in situations in which the vapor density of protons and alpha particles is large, that is, near the maximum temperature T_c. However, in such regions the electrons and the vapor will dominate the free energy and thus the neglect of the screening will not significantly alter the overall thermodynamic properties of the matter. We will neglect thermal (plasma) corrections to the Coulomb energy, but these also are of little significance except when the Coulomb parameter $\Gamma_C = Z^2e^2u^{1/3}/(r_N T) < 10$. Although Γ_C is about 10 in the core of a massive star prior to its gravitational collapse, it rapidly increases once collapse begins. Small Coulomb parameters may again be encountered during the formation of a protoneutron star, but in such situations the thermal energies of free nucleons will dominate the energies of the nuclei.

2.8. NUCLEI, BUBBLES AND OTHER PHASES

As was first discussed by Baym *et al.* [18]), it becomes energetically favorable near $\frac{1}{2}n_s$ for the nuclei to turn "inside-out", that is, for a system of relatively low-density neutron bubbles immersed in a dense proton-rich phase to replace the dense proton-rich nuclei immersed in a low-density neutron-gas phase. In the special case of three-dimensional bubbles, the total baryon free-energy density will still take the form of eq. (2.1), but F_o will now refer to the nucleons inside the bubble, the finite-size terms of F_N will refer to the bubble, and the bulk part of F_N will refer to the dense matter outside the bubble. Alpha particles will be confined to the region inside the bubbles. Letting u remain the filling factor of the dense phase, x_i and n_i the proton fraction and nucleon density of the dense phase, and V_N the volume occupied by the dense phase, F_N can be written as

$$F_N = n_i[u f_{bulk}(n_i, x_i, T) + (1-u)(f_s + f_C + f_H)] \qquad \text{bubbles}\,. \tag{2.35}$$

The surface and Coulomb terms will in this case become

$$f_s = \frac{3\sigma(x_i, T)}{r_B n_i}\,, \tag{2.36a}$$

$$f_C = \tfrac{4}{5}\pi e^2 x_i^2 r_B^2 n_i D(1-u)\,, \tag{2.36b}$$

where $D(1-u) \equiv 1 - \frac{3}{2}(1-u)^{1/3} + \frac{1}{2}(1-u)$ and r_B is the radius of the bubble. It is

seen that the bubble surface and Coulomb energy densities are obtained by replacing u in the nuclear surface and Coulomb energy densities ($un_i f_s$ and $un_i f_C$, respectively) by $1-u$.

Thus, in the absence of the effects of compression, curvature and translation, the transition between nuclei and bubbles would occur at exactly $u=\frac{1}{2}$, which corresponds to the density $\frac{1}{2}n_s$. Ravenhall *et al.* [20]) showed that several additional distinct phases of rod-, tube- or plate-like matter might also be energetically preferred, beginning at densities as low as $\frac{1}{10}n_s$. Moreover, it is unreasonable to expect that the nuclei will remain spherical in the subnuclear regime. Undoubtedly, the actual situation is quite complicated in this regime; a mixture of a number of phases of matter will exist at densities just below n_s.

It is thus unrealistic to describe matter via the procession of simple phases we have referred to as "nuclei", "bubbles" and "bulk" as the density is raised. We will include such distortions in the nuclear shape by introducing shape parameters for both the surface and Coulomb energies. These shape parameters will be assumed to depend only upon u, the filling factor of the dense phase, and not upon the underlying nuclear force, upon Y_e, or upon T. We assume that the generalized surface and Coulomb energy densities are

$$F_s=\frac{3\sigma}{r}s(u)\,,$$

$$F_C=\tfrac{4}{5}\pi e^2 x_i^2 n_i^2 r^2 c(u)\,, \tag{2.37}$$

where $s(u)$ and $c(u)$ are the shape parameters and r represents the generalized nuclear size. For example, for three-dimensional spheres, r is equivalent to either r_N or r_B, depending upon whether the energetically favored shape is nuclei or bubbles; for the one-dimensional configuration, r represents the sum of the thickness of the slabs.

The functions s and c are chosen to simulate the gradual transition from nuclei to bubbles as in the scheme of Ravenhall *et al.* [20]). If we could assume that the only nuclear energy terms that will depend upon r are the surface and Coulomb energies F_s and F_C, then it becomes straightforward to determine r as a function of the other nuclear variables (see eq. (3.2a) below). The bulk energy density $F_{\mathrm{bulk},i}$ is, of course, independent of r, but the translational energy density, F_H, is not. However, F_H is generally small compared to the other nuclear energies, and we will therefore approximate F_H so that it is independent of r (see the next section). Assuming that only F_s and F_C depend upon r, minimization of F_s+F_C with respect to r will result in $F_s=2F_c$, which is the nuclear virial theorem of Baym *et al.* [18]). This equation may be solved for r:

$$r=\left[\frac{15\sigma s(u)}{8\pi e^2 x_i^2 n_i^2 c(u)}\right]^{1/3}\equiv\frac{9\sigma}{2\beta}\left[\frac{s(u)}{c(u)}\right]^{1/3}, \tag{2.38}$$

which defines the quantity β. The sum $F_s + F_C$ may be expressed as

$$F_s + F_C = \beta[c(u)s(u)^2]^{1/3} \equiv \beta \mathscr{D}(u), \tag{2.39}$$

which defines $\mathscr{D}$.

In the low density (nuclei) limit, in which $u \to 0$, we have from eqs. (2.26) and (2.34) that $\mathscr{D}(u) \to u[D(u)]^{1/3}$; in the opposite (bubble) limit, $u \to 1$, we have from eqs. (2.35) and (2.36b) that $\mathscr{D}(u) \to (1-u)[D(1-u)]^{1/3}$. We seek an analytical interpolation for $\mathscr{D}$ to connect these limits and to accurately represent, at zero temperature, the results of Ravenhall *et al.* [20]).

Cooperstein and Baron [12]) have bridged these regimes with the expression

$$\mathscr{D}(u) = u(1-u)([D(u)]^{1/3} + [D(1-u)]^{1/3}), \tag{2.40}$$

which has the right functional and derivative limits. However, this particular expression overestimates the finite-size energy by between 5% and 8% in the interval $0.008 < u < 1.0$, compared to the results of ref. [20]). Moreover, the Coulomb lattice pressure derived from eq. (2.40) differs from that of ref. [20]) by as much as 20%, even at relatively low densities ($u \simeq 0.01$) where the expression $\mathscr{D} = uD^{1/3}$ is "exact" [see fig. 2]. One can compare this to the situation in which the bubble phase is neglected altogether (i.e., using $\mathscr{D} = uD^{1/3}$ throughout): the finite-size energy is then overestimated by less than 5% for $u < 0.4$ and by more than 15% for $u > 0.7$; but the lattice pressure is better approximated than by using eq. (2.40) as long as $u < 0.6$. Overall, a smaller error would be made, except in the narrow region $0.6 < u < 0.8$, by ignoring altogether the effect of the bubbles and other distorted nuclear shapes as given by eq. (2.40). But it is this latter regime that is important in fixing the lower boundary of the phase transition to uniform nuclear matter.

We have found a more accurate analytic formula that better describes the energy and pressure:

$$\mathscr{D}(u) = u(1-u)\frac{(1-u)[D(u)]^{1/3} + u[D(1-u)]^{1/3}}{u^2 + (1-u)^2 + 0.6u^2(1-u)^2}. \tag{2.41}$$

The factor of 0.6 in the denominator is an adjustable parameter determined by minimizing the differences in the energy and pressure compared to the more sophisticated calculation of Ravenhall *et al.* [20]). Eq. (2.41) has a maximum error in the finite-size energy and pressure of 1% and 4%, respectively, compared to ref. [20]), as displayed in fig. 2. It is important to emphasize that the u dependence in eq. (2.41) represents the result of competition among various phases of finite nuclei, and, at least in the approach of Ravenhall *et al.*, does not depend on the nuclear force parameters such as the incompressibility or the nuclear level density. It is important to note that thermal corrections to the Coulomb energy are not included; if they were, $\mathscr{D}$ would also become temperature dependent. Because $\Gamma_C \gg 1$ in almost all situations, this is a fair approximation.

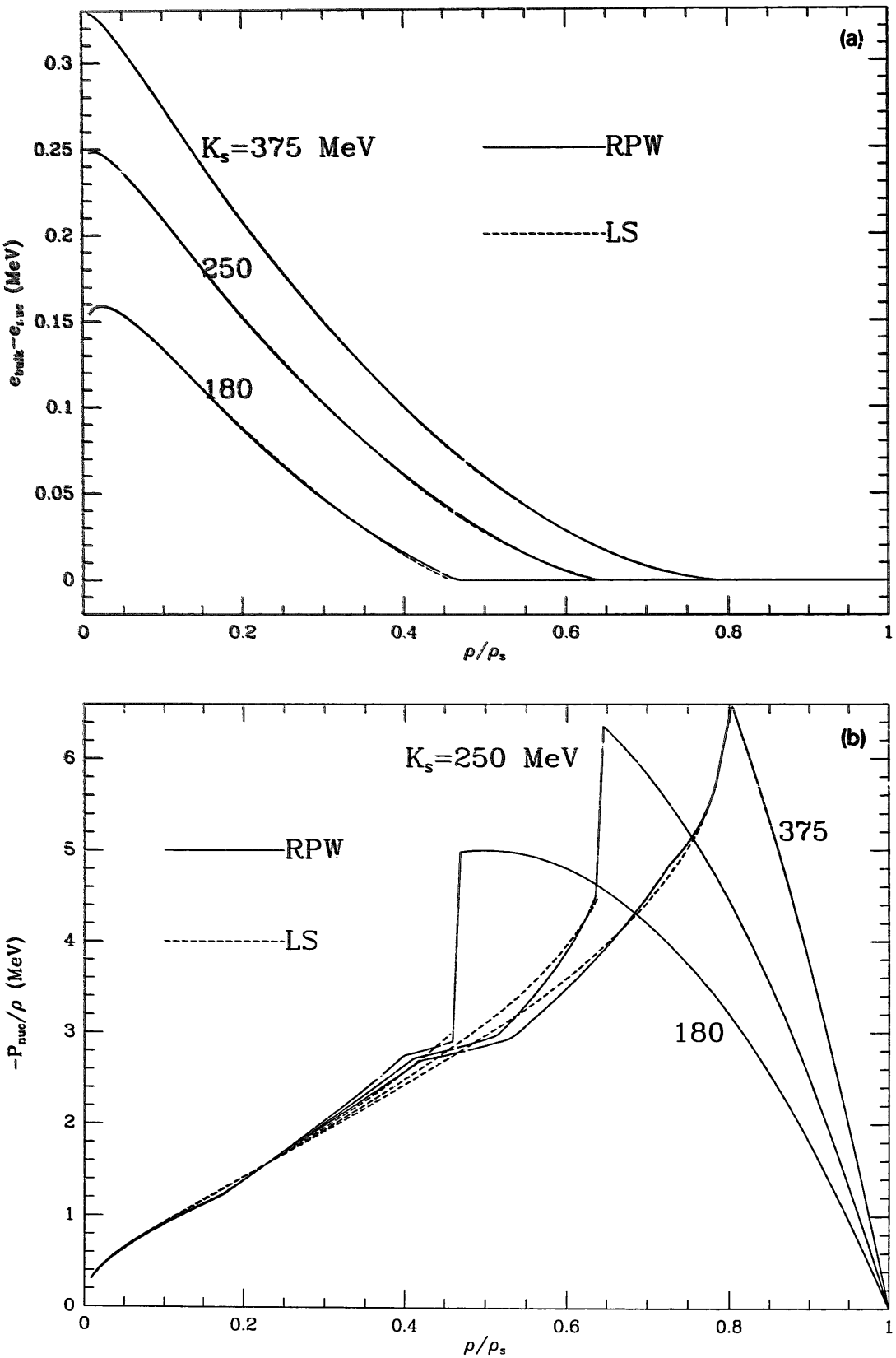

Fig. 2. Baryon energy and baryon pressure for cold symmetric matter. Solid curves are from Ravenhall *et al.* [20]); dashed curves are obtained from eq. (2.41). (a) Difference of energy per baryon of uniform matter and nuclei phases. (b) Baryon pressure/density ratio.

Our expression for the nuclear energy cannot, in general, be used all the way to $u = 1$. As demonstrated in sect. 3.3, a phase transition to bulk matter still exists, and this occurs for $u < 1$. The phase boundary is determined by a Maxwell construction between the nuclei phase and the uniform matter phase, which occurs, depending on Y_e, T and the nuclear force parameters around $u \simeq 0.5$–0.99.

2.9. TRANSLATIONAL ENERGY OF HEAVY NUCLEI

If we were to assume that the heavy nuclei were point particles of mass $A = \frac{4}{3}\pi r^3 n_i$, with a statistical weight factor of unity, then the translational free-energy density would be

$$F_H = \frac{u n_i}{A}(\mu_H - T) \tag{2.42}$$

where

$$\mu_H = T \ln\left(\frac{n_N}{n_Q A^{3/2}}\right) \tag{2.43}$$

is the translational chemical potential of the heavy nuclei. LLPR included three corrections to this formula: an effective mass, or "backflow", correction, an excluded volume correction, and a temperature reduction factor. We will not include the first two effects, which take into account that the nucleus is not immersed in a vacuum and that the volume available for translation is reduced from the entire cell volume $V_c = 1/n_N$. We will, however, multiply the translational free energy by a factor h, to account for the fact that considering the center-of-mass motion of the heavy nuclei to be that of a point particle is not valid near T_c.

There is an inherent dependence on the nuclear size in the translational energy, which will complicate the equilibrium condition obtained from minimizing the free energy with respect to the size, r. This condition may be solved explicitly, however, if one can ignore this size dependence, and in this spirit, we will simply assume that *in the translational energy only* $A = A_o$, a constant we choose to be 60. We emphasize that this approximation is made *only* in the translational energy and nowhere else. This approximation is most unrealistic at high temperatures, where translation may reduce the nuclear size by 25% or more. However, the effect on the pressure and chemical potentials is always negligible, and we can justify this approximation on this basis. In applications in which a more precise evaluation of the nuclear size is needed, as perhaps in calculations of the coherent neutrino-nuclear scattering mean free path or the nuclear electron capture rate, corrections to A which incorporate translational effects could be developed.

In contrast to LLPR, who neglected the translational contributions to the energy of the bubble phase, we will employ eq. (2.42) for all shapes (and, therefore, all values of u), by using the interpolation $n_N = u(1-u)n_i/A_o$ in the definitions of F_H

and μ_H. Since the translational contributions in the limit $u \to 1$ (the bubble limit) are very small, this procedure will have little effect on the results, but will avoid the small unphysical discontinuity that arises from the total neglect of the bubble translational energy. Thus, in summary, the total translational free-energy density is

$$F_H = u(1-u)n_i f_H = \frac{u(1-u)n_i}{A_o} h(\mu_H - T)$$

$$= \frac{u(1-u)n_i}{A_o} h\left[T \ln\left(\frac{u(1-u)n_i}{n_Q A_o^{5/2}}\right) - T\right]. \tag{2.44}$$

There will be no contribution to the equilibrium equation from the translational energy when F is minimized with respect to r.

3. Equilibrium conditions

3.1. MINIMIZATION OF THE FREE ENERGY

In general, the free-energy density must be minimized to find the equilibrium state. There are seven internal variables: x_i, n_i, u, r, n_{no}, n_{po}, and n_α. We must also include the conservation equations for baryon number and charge. These equations are

$$n = un_i + (1-u)[4n_\alpha + (n_{no} + n_{po})(1 - n_\alpha v_\alpha)], \tag{3.1a}$$

$$nY_e = ux_i n_i + (1-u)[2n_\alpha + n_{po}(1 - n_\alpha v_\alpha)]. \tag{3.1b}$$

We may choose any five independent variables to carry out the minimization, and we have chosen r, n_i, x_i, u and n_α. Minimizing, in turn, the total free-energy density F with respect to each of these variables, subject to the constraints (3.1), results in the following equilibrium equations:

$$0 = \frac{\partial F}{\partial r}: \quad r = \frac{9\sigma}{2\beta}\left(\frac{s(u)}{c(u)}\right)^{1/3}, \tag{3.2a}$$

$$0 = -\frac{1}{un_i}\frac{\partial F}{\partial x_i}: \quad \hat{\mu}_i - \frac{2\beta\mathscr{D}}{3un_i}\left(\frac{1}{x_i} + \frac{\sigma'}{\sigma}\right) - \frac{(1-\mu)}{A_o} h'(\mu_H - T) = \hat{\mu}_o, \tag{3.2b}$$

$$0 = \frac{\partial F}{\partial n_i} - \frac{x_i}{n_i}\frac{\partial F}{\partial x_i}: \quad \mu_{ni} - \frac{2\beta\mathscr{D}x_i\sigma'}{3un_i\sigma} + \frac{(1-u)}{A_o}[h\mu_H - x_i h'(\mu_H - T)] = \mu_{no}, \tag{3.2c}$$

$$0 = \frac{n_i}{u}\frac{\partial F}{\partial n_i} - \frac{\partial F}{\partial u}: \quad P_i + \beta\left(\frac{2\mathscr{D}}{3u} - \mathscr{D}'\right) + \frac{un_i}{A_o} h\mu_H = P_o + P_\alpha, \tag{3.2d}$$

$$0 = \frac{\partial F}{\partial n_\alpha}: \quad \mu_\alpha = 2(\mu_{no} - \mu_{po}) + B_\alpha - P_o v_\alpha. \tag{3.2e}$$

The functions β and $\mathscr{D}(u)$ have been used to simplify eqs. (3.2b)-(3.2d). In eqs. (3.2) we have also used the notation $\hat{\mu} \equiv \mu_n - \mu_p$, $\mathscr{D}' = \partial\mathscr{D}(u)/\partial u$, and $h' = \partial h/\partial x_i$. These relations are simply interpreted as the equation optimizing the nuclear size, the equations describing the chemical potential and pressure equilibria of the two fluids, and an equation describing the chemical equilibrium of the alpha particles with the nucleons.

Eq. (3.2e) now makes clear why the inclusion of the volume excluded by the α-particles is necessary. At supernuclear densities, the potential energies V_n and V_p become positive, reflecting the repulsive multi-body term ($cn^{1+\delta}$ in eq. (2.8)). This forces μ_n and μ_p to become more positive, and if the $P_o v_\alpha$ term in eq. (3.2e) was neglected, μ_α would also become large: α-particles would dominate at these densities. However, P_o also becomes large and positive, and forces down the values of μ_α and n_α. Therefore, the α-particle fraction actually tends to zero in the high-density limit.

The nuclear size r has been effectively eliminated from the equilibrium equations by the use of eq. (2.41), and it is not needed to determine the thermodynamic properties of the matter. Note that r does not appear in eqs. (3.2b)-(3.2e). However, the nuclear size is required in some applications, such as the calculation of the neutrino opacities. To determine r, we need to specify the combination $s(u)/c(u)$, while $\mathscr{D}(u)$ represents the combination $[c(u)s(u)^2]^{1/3}$. A reasonable approximation is to use the simple interpolation $s(u) = u(1-u)$, which leads to

$$r \simeq \frac{9\sigma u(1-u)}{2\beta\mathscr{D}}, \tag{3.3}$$

which has the correct limits in the cases $u \to 0$ and $u \to 1$. This expression is a moderate overestimate of r in the vicinity of $u \approx \frac{1}{2}$. Note that the use of an approximate value for r does not lead to any thermodynamic inconsistencies.

3.2. THERMODYNAMIC QUANTITIES

We may calculate the other thermodynamic quantities from F using eqs. (2.2). We obtain

$$\mu_e - \frac{\partial F/n}{\partial Y_e} = \hat{\mu} = \hat{\mu}_o, \tag{3.4a}$$

$$\frac{\partial F}{\partial n} - \frac{Y_e}{n}\frac{\partial F}{\partial Y_e} = \mu_n = \mu_{no}, \tag{3.4b}$$

$$-\frac{\partial F}{\partial T} = ns = un_i s_i - \left(\frac{2\beta\mathscr{D}}{3h} + \frac{F_H}{h}\right)\frac{\partial h}{\partial T} + \frac{u(1-u)n_i h}{A_o}\left(\tfrac{5}{2} - \mu_H/T\right)$$
$$+ (1-u)(1-n_\alpha v_\alpha)n_o s_o + (1-u)n_\alpha\left(\tfrac{5}{2} - \mu_\alpha/T\right) + n(s_e + s_\gamma), \tag{3.4c}$$

$$n^2\frac{\partial F/n}{\partial n} = P = P_o + P_\alpha - \beta(\mathscr{D} - u\mathscr{D}') + \frac{un_i}{A_o}h[T(1-u) - u\mu_H] + P_e + P_\gamma, \quad (3.4d)$$

$$= P_i + \beta\mathscr{D}\left[\frac{2}{3u} - 1 - \frac{\mathscr{D}'}{\mathscr{D}}(1-u)\right] + \frac{u(1-u)n_i}{A_o}h(\mu_H + T) + P_e + P_\gamma. \quad (3.4e)$$

The last two equations were derived by incorporating appropriate combinations of the equilibrium conditions, eq. (3.2). The terms P_e, s_e and P_γ, s_γ refer to the electrons and photons, respectively (see appendix C). The Coulomb lattice contributions to the pressure are clearly seen in eq. (3.4d). The major contribution to the nuclear translational pressure is just $hun_iT/A_o \simeq n_N T$, as expected for a Maxwell–Boltzmann gas of nuclei. It should be noted that, in the limit $u \to 1$, the Coulomb and translational contributions in eq. (3.4e) vanish, while in the limit $u \to 0$, the contributions in eq. (3.4d) vanish. These properties guarantee that thermodynamic variables are continuous as one goes from the two-phase (nuclei plus vapor) regime to the one-phase (bulk fluid or vapor plus alphas) regime.

3.3. PHASE TRANSITION BETWEEN NUCLEI AND UNIFORM MATTER

One can easily demonstrate that a transition from the nuclei phase to the uniform matter phase occurs below nuclear density. Write the finite-size energy density in the form $\beta\mathscr{D}(u)$, *viz.*, eq. (2.41). For the bubble phase, therefore, we have $\mathscr{D}(u) = (1-u)[D(1-u)]^{1/3}$. The uniform matter's energy per baryon can be expressed using the customary expansion about the saturation density:

$$E_{\rm bulk}(n)/n \simeq -16 + \tfrac{1}{18}K_s(n/n_s - 1)^2, \quad (3.5)$$

where K_s is the incompressibility parameter. If we ignore the existence of vapor nucleons inside bubbles, and the slight compression of the dense phase due to the finite-size energy terms, we have $n = un_i$ and $n_i = n_s$. Thus the bulk energy per particle for the bubble system is $f_i = -16$ MeV. Equating the energy per baryon of the bubble phase (i.e., $f_i + \beta\mathscr{D}/n$) with that of the uniform matter phase (eq. (3.5)) gives an implicit expression for the mid-point of the phase transition (the leptonic energies are the same for both phases and may be ignored):

$$u \simeq 1 - \sqrt{\frac{18\beta\mathscr{D}(u)}{uK_sn_s}} = 1 - \frac{18\beta[D(1-u)]^{1/3}}{uK_sn_s}, \quad (3.6)$$

which shows that, besides the obvious solution $u = 1$, a solution with $u < 1$ also occurs. With $\beta/n_i \simeq 7.1$ MeV and $\frac{1}{18}K_s \simeq 20$ MeV, we find $u \simeq 0.72$. Clearly, the nuclear force parameters, the temperature and the composition of the matter will together determine the phase boundaries.

We will assume that matter is in thermal equilibrium. Nuclear and electromagnetic rates are extremely rapid compared to dynamical times in any realistic application.

Thus, matter on both sides of the phase boundary will have the same temperature, not the same entropy. The densities defining the phase-transition boundaries, n_ℓ and n_h, are thus found by minimizing the free-energy density in the phase-transition region with respect to these densities. Denoting the total free-energy density within the phase boundaries by $F(n, n_\ell, n_h, Y_e, T)$, the free-energy density at the low-density boundary n_ℓ by $F_\ell(n_\ell, Y_e, T)$, and the free-energy density at the high-density boundary n_h by $F_h(n_h, Y_e, T)$, we can write

$$F = vF_h + (1-v)F_\ell , \tag{3.7}$$

where the volume fraction occupied by the denser phase is $v = (n-n_\ell)/(n_h-n_\ell)$. The minimization conditions

$$\left.\frac{\partial F}{\partial n_\ell}\right|_{n_h,n,Y_e,T} = \left.\frac{\partial F}{\partial n_h}\right|_{n_\ell,n,Y_e,T} = 0 \tag{3.8}$$

give the expected results

$$P = P_\ell = P_h = \frac{n_\ell F_h - n_h F_\ell}{n_h - n_\ell} = \text{const},$$

$$\mu = \mu_\ell = \mu_h = \frac{F_h - F_\ell}{n_h - n_\ell} = \text{const} \qquad \text{for } n_\ell \leq n \leq n_h . \tag{3.9}$$

Here, the pressure is defined by eq. (2.2), i.e., $P = \mu n - F$, and the Gibbs free energy per baryon is $\mu = \partial F/\partial n|_{Y_e,T}$. Eq. (3.9) is just the standard Maxwell construction and provides two equations that may be used to solve for n_ℓ and n_h. For a given set of nuclear parameters, n_ℓ and n_h vary rather slowly with Y_e and T, and they are tabulated and stored. When densities intermediate to n_ℓ and n_h are encountered, the values of the thermodynamic variables can be established from the Maxwell construction, using the minimization conditions eq. (3.8):

$$P = n\left.\frac{\partial F}{\partial n}\right|_{Y_e,T} - F = P_\ell = P_h ,$$

$$F = F_\ell + \mu_\ell (n - n_\ell) ,$$

$$\hat{\mu} - \mu_e = -\frac{1}{n}\left.\frac{\partial F}{\partial Y_e}\right|_{n,T} = (1-v)(\hat{\mu}_\ell - \mu_{e\ell}) + v(\hat{\mu}_h - \mu_{eh}) ,$$

$$\mu_n = \mu_\ell + Y_e(\hat{\mu} - \mu_e) ,$$

$$ns = -\left.\frac{\partial F}{\partial T}\right|_{n,Y_e} = (1-v)s_\ell n_\ell + v s_h n_h . \tag{3.10}$$

A typical situation is presented in fig. 6, for our "standard" nuclear parameter set (see sect. 5). The phase boundaries, including the Maxwell construction boundaries, are shown by the curves. These boundaries merge at high temperatures, and the transition is marked by a single curve at which the free energies of the two

phases become the same. The boundary curve continues through the maximum in temperature to lower densities, where it smoothly joins the nuclear dissociation curve (in this figure, this curve is defined by the mass fraction of nuclei $X_H = 10^{-4}$). As expected, the phase boundaries shift to lower temperatures and densities as Y_e is decreased.

4. Method of solution

As they stand, the equilibrium equations (3.2) and the conservation equations (3.1) are not amenable to an exact solution involving less than a three-dimensional iteration scheme because only four of the variables u, n_i, x_i, r, n_{no}, n_{po} and n_α can be expressed as a closed function of the others. The chemical potential and pressure equilibrium equations, eqs. (3.2b)-(3.2d), are not simple analytic relations. However, one can obtain straightforward analytic derivatives of these equations with respect to the three remaining free variables (see appendix A). Thus a full Newton-Raphson iteration scheme is practical. We pursue this method in this section.

In many applications, the input thermodynamic variables will not be the standard set (n, Y_e, T), but may include the pressure, internal energy, and/or the entropy. It is straightforward to generalize the computation of the EOS for alternate input variables by using a Newton-Raphson iteration. This can either be done separately from the solution of the equilibrium equations, in which case there will be a set of two nested iterations, or be done simultaneously with the solution of the equilibrium equations, in which case the dimensionality of the iteration scheme is increased. In either case, it is necessary to have derivatives of the alternate variables with respect to the standard ones. These can be computed analytically, and are given in appendix B.

4.1. NUCLEI IN EQUILIBRIUM WITH THE VAPOR OF NUCLEONS AND α-PARTICLES

Let us first discuss the choice of variables to be used to solve the equilibrium conditions eq. (3.2). There are a total of seven internal variables: x_i, n_i, u, r, n_{no}, n_{po} and n_α. It has already been emphasized that r can be eliminated from this system through the first equilibrium condition eq. (3.2a), which corresponds to using eq. (2.41) for the sum of the surface and Coulomb energies. Next, we note that the mass and charge balance equations (3.1) can be trivially solved for u and x_i in terms of the other variables:

$$u = \frac{n - (n_{no} + n_{po})(1 - n_\alpha v_\alpha) - 4n_\alpha}{n_i - (n_{no} + n_{po})(1 - n_\alpha v_\alpha) - 4n_\alpha}, \tag{4.1a}$$

$$x_i = \frac{nY_e(n_i - (n_{no} + n_{po})(1 - n_\alpha v_\alpha) - 4n_\alpha) - (n_{po}(1 - n_\alpha v_\alpha) + 2n_\alpha)(n_i - n)}{n_i(n - (n_{no} + n_{po})(1 - n_\alpha v_\alpha) - 4n_\alpha)}. \tag{4.1b}$$

Furthermore, n_α is an explicit function of n_{no} and n_{po} through eqs. (3.2e) and (2.25):

$$n_\alpha = 8 n_Q \exp\left[\frac{B_\alpha + P_o v_\alpha}{T} + 2(\eta_{no} + V_{no}/T + \eta_{po} + V_{po}/T)\right]. \tag{4.2}$$

We note from eqs. (2.15) and (2.18) that the degeneracy parameters η_{no} and η_{po}, the potential energies V_{no} and V_{po}, and the pressure P_o are functions of the nucleon number densities and temperature alone. As a result, u and x_i are established as explicit functions of the three remaining variables n_i, n_{no} and n_{po}. The values of these three independent variables can be found by iteration, using the three equilibrium conditions, eqs. (3.2b)–(3.2d).

There are good reasons why u and x_i are used as dependent variables, and n_i as the independent variable, as opposed to other possible choices. First, the choice of n_i and x_i as dependent variables is poor because they are relatively slowly varying over the domain of n, Y_e, T space, while u, which would be the independent variable, spans the entire range 0–1. This makes u undesirable as the independent variable. Secondly, suppose we had chosen to use, instead, the pair u and n_i as dependent variables, so that x_i would become the independent variable. The requisite equations would be

$$1 - u = \frac{n(Y_e - x_i)}{2n_\alpha(1-2x_i) + (1 - n_\alpha v_\alpha)(n_{po} - x_i(n_{no} + n_{po}))}, \tag{4.3a}$$

$$n_i = \frac{n - (n_{no} + n_{po})(1-u) + 4n_\alpha(1-u)}{u}. \tag{4.3b}$$

The first of these has the drawback of going to a finite zero over zero limit when the mass fraction of nuclei is close to one, for any u. This property makes x_i undesirable as the independent variable. Note that eqs. (4.1) have well-defined limits in this case.

It should be mentioned that a potential difficulty exists with eq. (4.1b) in the limit when nuclei disappear ($u \to 0$), since the denominator, which is proportional to u, becomes small. However, it may be shown that the variable x_i is approximately bounded within the range $0.8\,Y_e - 0.5$. The existence of these bounds can be used to remove the potential convergence problems.

In practice, it is desirable to employ the logarithms of the number densities n_{no}, n_{po} as independent variables, instead of the number densities themselves. There are regimes, especially at lower temperatures, in which the number densities can become very small and rapidly varying, and the values of the number densities are not especially relevant in the mass and charge conservation equations. But the degeneracy parameters (or chemical potentials) are always relevant quantities because of the equilibrium conditions, and these are proportional to the logarithms of the densities in this limit. In fact, the quantities $\log(n_{io}/T^{3/2})$ are especially

slowly varying with changes in temperature, and represent good choices for the independent variables. For nuclear interactions characterized by $m_i^* = m$ (i.e., $\alpha_1 = \alpha_2 = 0$), it is even more convenient to use $T\eta_{no}$ and $T\eta_{po}$ as the independent variables, since each η_i is a function only of the corresponding n_i and T. In the non-degenerate limit, in which the number density n_{io} becomes small, $\eta_{io} \propto \ln(n_{io}/T^{3/2})$. Thus, although the following discussion and appendices B and C will assume that the set of independent variables is $z_j = (n_i, n_{no}, n_{po})$, it is trivial to modify these expressions if the alternate sets $z_j = (n_i, \ln(n_{no}/T^{3/2}), \ln(n_{po}/T^{3/2}))$ or $z_j = (n_i, T\eta_{no}, T\eta_{po})$ are used instead.

The three equilibrium equations eqs. (3.2b)-(3.2d) must be solved numerically for the three chosen variables. We write these three equations as

$$A_1 = P_i - B_1 - P_o - P_\alpha ,$$

$$A_2 = \mu_{ni} - B_2 - \mu_{no} ,$$

$$A_3 = \mu_{pi} - B_3 - \mu_{po} . \tag{4.4}$$

Here, using eqs. (3.2), we find

$$B_1 = \beta\left(\mathscr{D}' - \frac{2\mathscr{D}}{3u}\right) - \frac{un_i}{A_o} h\mu_H ,$$

$$B_2 = \frac{2\beta\mathscr{D}x_i\sigma'}{3un_i\sigma} - \frac{(1-u)}{A_o}[h\mu_H - x_i h'(\mu_H - T)] ,$$

$$B_3 = \frac{2\beta\mathscr{D}}{3un_i}\left(\frac{\sigma'}{\sigma}(x_i - 1) - \frac{1}{x_i}\right) - \frac{(1-u)}{A_o}[h\mu_H + h'(1-x_i)(\mu_H - T)] . \tag{4.5}$$

The essence of the Newton-Raphson method is to update the values of n_i, n_{no} and n_{po} from previous estimates by using the increments

$$\delta z_j = -(D_{kj})^{-1} A_k , \qquad j, k = 1, 3 \tag{4.6}$$

where

$$D_{kj} = \left(\frac{\partial A_k}{\partial z_j}\right) \tag{4.7}$$

is the matrix of derivatives, z_j is the set of independent variables, and there is implied summation in eq. (4.6). The elements of D_{kj} can be found analytically and are given in appendix A.

We summarize the computational method in the nuclei regime: initial guesses for n_i, n_{no} and n_{po}, are used. From them, x_i and u are determined from eq. (4.1). Now, all the quantities in eq. (4.4) may be evaluated. New guesses are forthcoming after a Newton-Raphson step, eq. (4.6).

4.2. DISSOCIATED REGIME: NUCLEONS AND α-PARTICLES ONLY

At sufficiently high temperature for a given density below the saturation density n_s, the nuclei completely dissociate and the equilibrium conditions eqs. (3.2a)–(3.2d) will no longer apply. However, the nucleon–alpha equilibrium eq. (3.2e) is still maintained. The same situation occurs above the phase transition to bulk matter, which occurs just below nuclear matter density. The $P_o v_\alpha$ term in eq. (3.2e) ensures that α-particles disappear at high densities. Although this equilibrium can be written as a quartic equation in $n_\alpha^{1/2}$ if the nucleon gas is ideal, at densities above $0.001 n_s$, this is not satisfactory. We outline here a general one-dimensional Newton–Raphson solution for the nucleon–alpha regime, that is actually more efficient than the quartic solution in the ideal case.

For the independent variable we choose $X_p = n_{po}/n$. Then elimination of n_α from eqs. (3.1), with $u = 0$, yields

$$n_{no} = n\frac{X_p[2 - nv_\alpha(1 - Y_e)] + 2(1 - Y_e)}{2 - nv_\alpha Y_e}, \qquad n_{po} = nX_p. \tag{4.8}$$

With these values for n_{no} and n_{po}, the use of eq. (2.15) gives $\eta_{n,o}$ and η_{po}; eq. (2.12) gives μ_{no} and μ_{po}; eq. (3.2e) gives μ_α; and, finally, eq. (2.25) gives n_α. A one-dimensional iteration on the mass conservation equation $n = (n_{no} + n_{po})(1 - n_\alpha v_\alpha) + 4n_\alpha$ can then be used to solve for corrected values of X_p. In the situation in which n_α vanishes, the solution is trivial: $X_p \to Y_e$.

There is a technical problem in determining, for a given (n, T, Y_e) combination, whether or not nuclei exist. If nuclei do not exist, or their abundances are negligibly small, the three dimensional iteration described in the previous section will fail to converge. It is then simple, but rather inefficient, to switch from the three-dimensional nuclei solution to the one-dimensional alpha–nucleon iteration to find the equilibrium solution. Thus, increasing the temperature at fixed density and electron fraction forces the nuclear abundance to decrease, until, finally, nuclei completely disappear. However, going through the dissociation region in the opposite direction is not so straightforward, since one does not know *a priori* the temperature at which nuclei will reappear. One must attempt to solve the three dimensional iteration at each temperature as the temperature is decreased. When it finally converges, nuclei appear. This procedure is unnecessarily inefficient. For this reason, we have chosen to store the (n, T, Y_e) information for this boundary, defined as the locus of points for which the nuclei have a mass fraction of 0.01%, or for which the free energies of the phases with and without nuclei are equal. This boundary is computed by a separate program which calls the EOS code, and the data is stored in an ASCII file. A startup routine reads this file prior to the initial call to the EOS in order to initialize the array of boundary points, along with the array containing the phase boundaries of the Maxwell construction. This boundary and phase data is thus computed once and stored on disk. Of course, each time a new set of nuclear force

parameters is employed, these boundaries must be recomputed. Examples of these phase boundaries are discussed in the next section.

5. Results

We adopt the "standard" parameter set $K_s = 375$ MeV, $B = 16$ MeV, $S_v = 29.3$ MeV, $\sigma_s = 1.15$ MeV $\cdot$ fm^{-2}, $S_s = 45.8$ MeV, $n_s = 0.155$ fm^{-3} and $m^* = m$. The parameters T_{cc} and a_s are then established from eqs. (2.31) and (2.32). This parameter set, with the notable exception of m^*, is equivalent to the Skyrme I' set employed by LLPR. We will first identify what the major differences between our results with this parameter set and LLPR are, and then we present results with more realistic values of K_s and also compare with the results of CB.

In our description of the EOS, using the standard parameters, most of the thermodynamic properties obtained by LLPR are well-modeled, including the locations of phase boundaries, isobars and isoergs. Our choice of $m^* = m$ and our neglect of the neutron skin of the nucleus and the translational A dependences, lead to the only significant differences. We compare T, $\hat{\mu}$, and A along $s = 1$ and $s = 1.5$ adiabats in figs. 3-5.

The largest differences, as we now discuss, can be attributed to the choice of symmetry energy in the nuclear model. At low densities, it is straightforward to show that the symmetry-energy difference

$$A(1-2x_i)^2\left[\frac{S_v}{1+(S_s/S_v)A^{-1/3}}-(S_v-S_sA^{-1/3})\right] \tag{5.1}$$

between LLPR and this work leads to the chemical-potential differences

$$\Delta\mu_n = 2(1-2x_i)\left[\frac{S_v}{1+(S_s/S_v)A^{-1/3}}-(S_v-2x_iS_sA^{-1/3})\right],$$

$$\Delta\hat{\mu} = 4(1-2x_i)\left[\frac{S_v}{1+(S_s/S_v)A^{-1/3}}-(S_v-S_sA^{-1/3})\right]. \tag{5.2}$$

For $Y_e = 0.3$, $n \approx 10^{-4}$-10^{-5} fm^{-3} and $T < 1$ MeV, one finds $x_i \simeq 0.33$ and $A \simeq 100$, and eq. (5.2) implies that $\Delta\mu_n \simeq -0.6$ MeV and $\Delta\hat{\mu} \simeq 3.3$ MeV. This value for $\Delta\hat{\mu}$ agrees well with the results shown in fig. 4. Obviously, low density, low temperature values of the chemical potentials must agree with experimental information, which implies that one must take care to use a set (S_v, S_s) that is consistent with both the nuclear mass model and nuclear systematics. Thus, in our approach, in order to obtain the same value as LLPR for $\hat{\mu}$ for a laboratory nucleus like Fe, one should select a smaller value of S_s, about 33 MeV, if S_v is to remain unaltered.

A further consequence of a non-zero value for $\Delta\mu_n$ is that the mass fraction of neutrons, which are nondegenerate for these conditions, is a factor of $\exp \Delta\mu_n/T \sim 0.4$ less in our model than in LLPR. Since the entropy here is dominated by the external nucleon vapor (the s_o term in eq. (3.4c)), the temperature along the adiabat must be higher than for for LLPR, as shown in fig. 3.

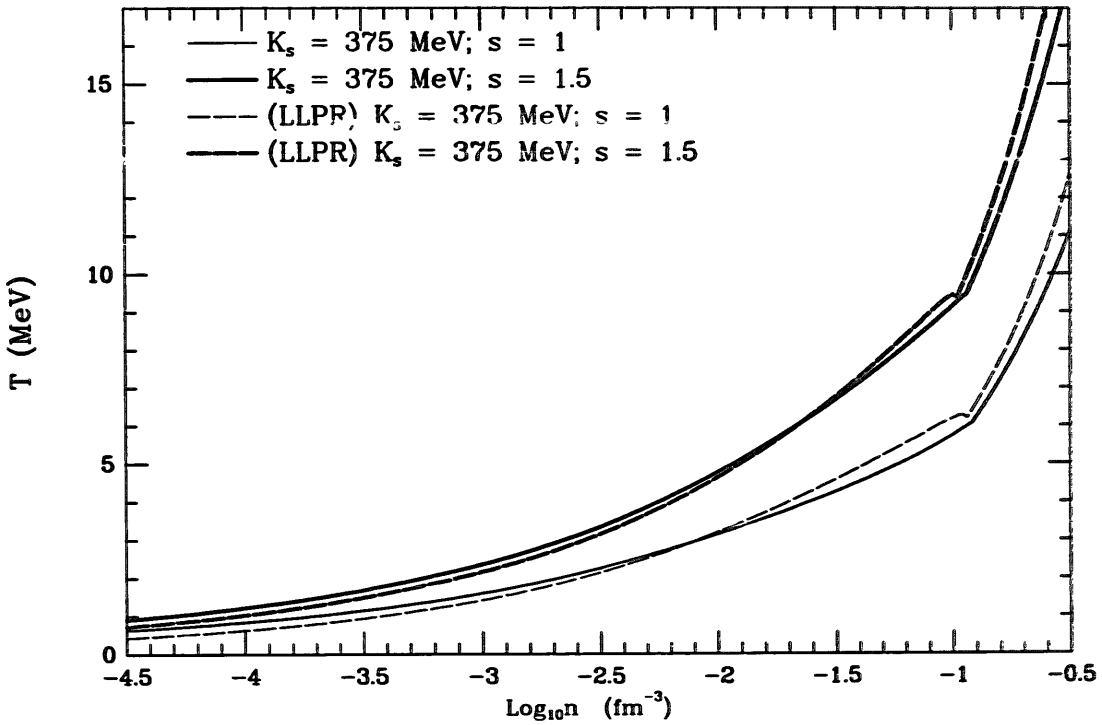

Fig. 3. Temperature along adiabats labelled by the entropy per baryon, for the case $Y_e = 0.3$.

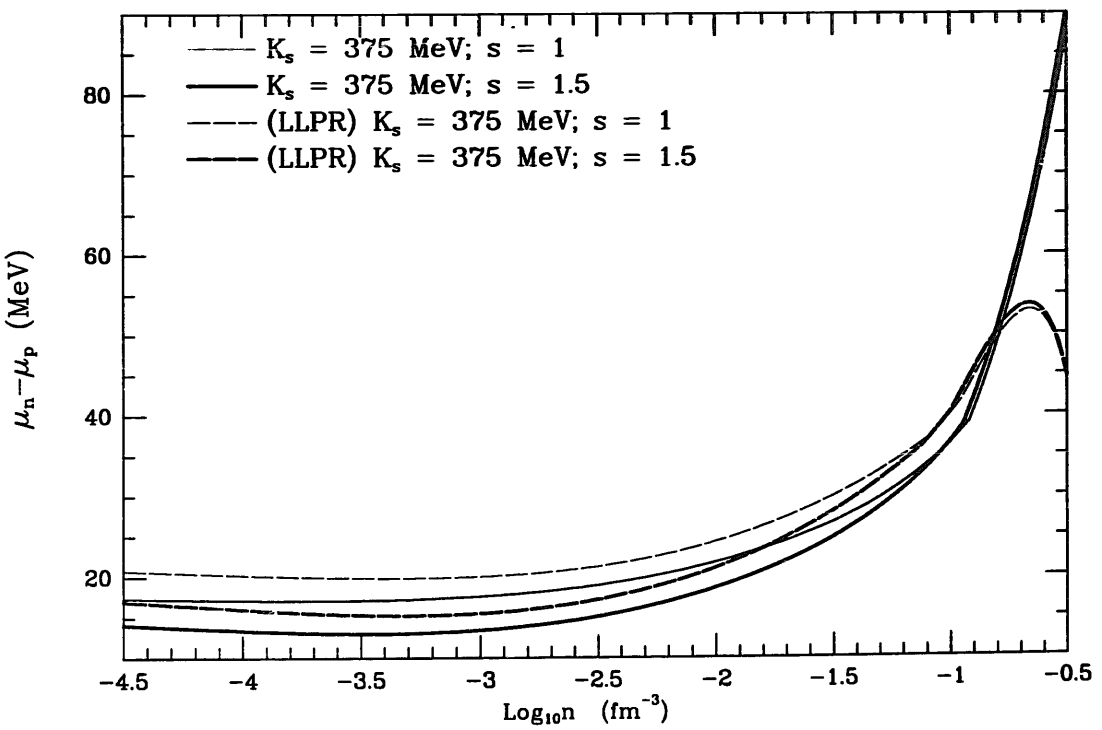

Fig. 4. Same as fig. 3, except $\hat{\mu} = \mu_n - \mu_p$ is displayed.

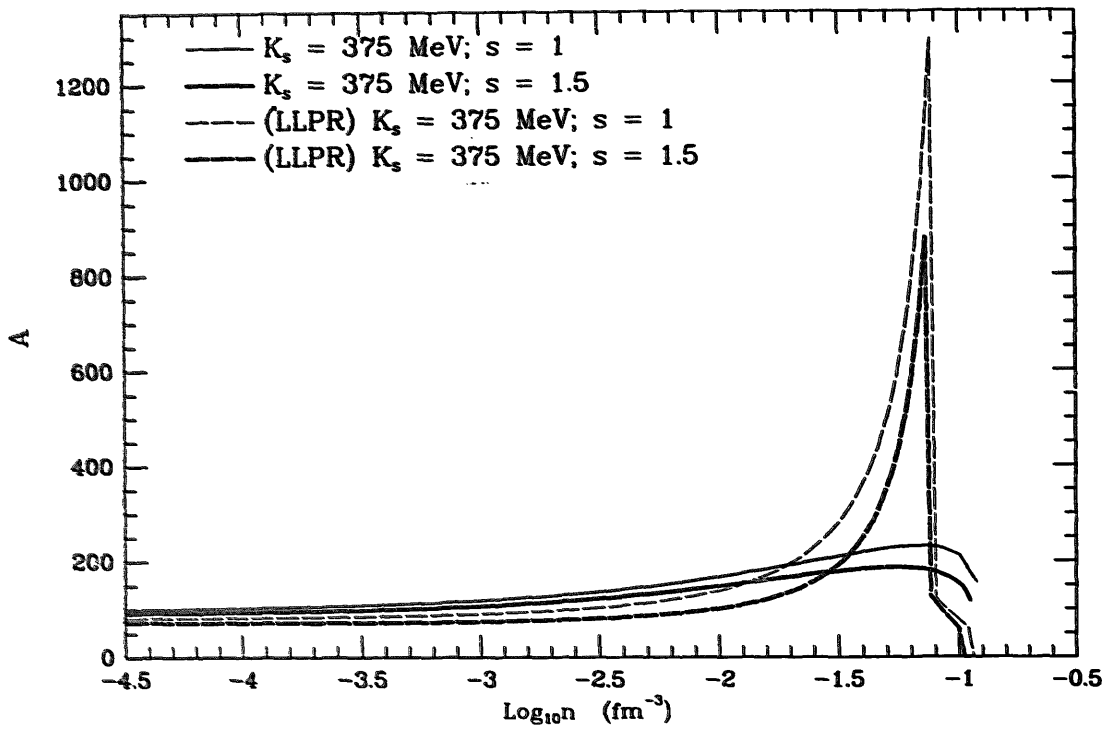

Fig. 5. Same as fig. 3, except nuclear mass number A is displayed. Curves terminate at the phase boundary.

At supernuclear densities, however, the nuclear specific heat, which is directly proportional to m^*, is larger in our model than in LLPR. Thus, as seen in fig. 3, at the highest densities, the temperature along adiabats becomes larger than in the model of LLPR. The chemical-potential behavior at high densities displayed in fig. 4 is more complicated, and depends upon the x dependence of the nucleon-nucleon force (i.e., eq. (2.8)). The bulk matter symmetry energy, and $\hat{\mu}$, of the nucleon-nucleon force used in this paper increase monotonically with density, as seen in fig. 4. However, the Skyrme I′ force employed by LLPR has the characteristic that the symmetry energy, and $\hat{\mu}$, begin to decrease beyond $1.5n_s$. This is due to the x dependence in the three-body interaction, which dominates above n_s. Unfortunately, at present, there is little or no experimental information that can be used to discriminate between these density dependencies.

Lastly, fig. 5 displays the nuclear mass number A along these adiabats. Below densities at which nuclear shape variations may be important, our approach is seen to overestimate A, chiefly because of the neglect of translational effects. However, as the transition to bulk matter is approached, our A values shrink below those of LLPR due to our inclusion of the aforementioned shape variations.

We next consider varying the nuclear compression modulus K_s. This not only affects how baryon pressure changes with density, but also affects the critical temperature, the phase boundaries, and the nuclear specific heat. Fig. 6 shows the nuclear phase boundary and fig. 7 adiabats and isoergs for the cases $K_s = 375$, 220 and 180 MeV. In accord with eq. (2.31) both adiabats and phase boundaries are at

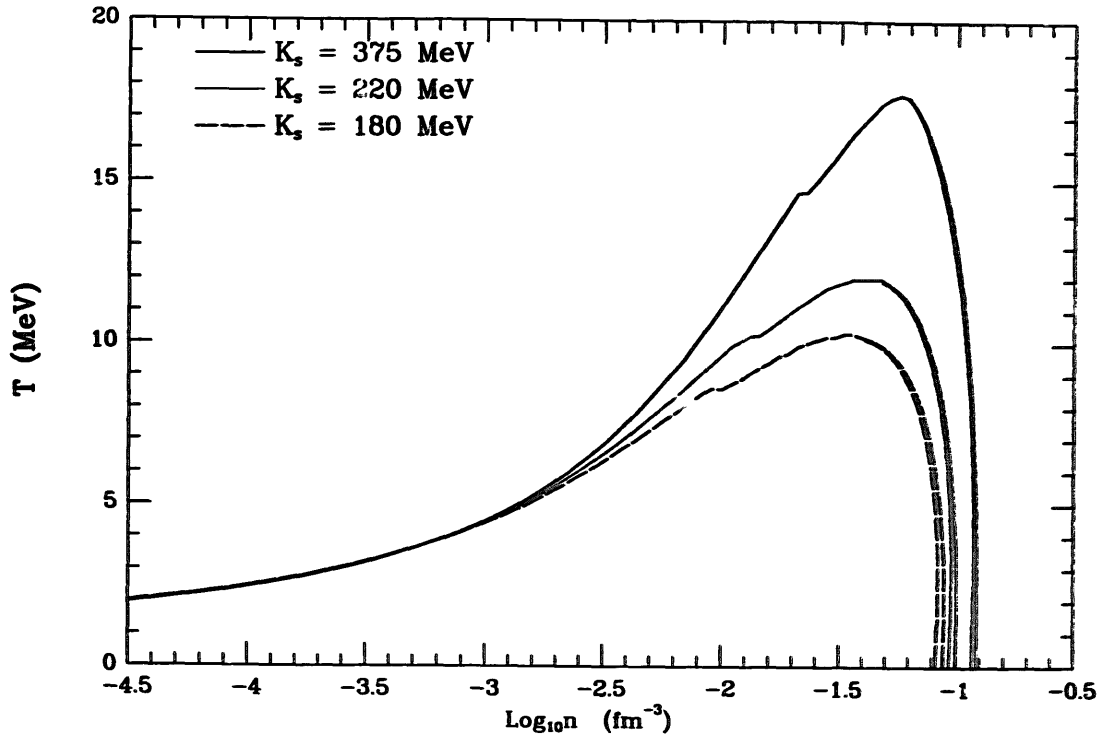

Fig. 6. Phase boundaries between uniform matter and nuclei for the case $Y_e = 0.3$ and for selected values of the incompressibility K_s.

lower temperatures for smaller values of K_s. However, above phase transition densities, the temperature along adiabats is independent of K_s. This is because, according to eqs. (2.9), (2.10) and (2.14)–(2.16), s_{bulk} depends only on n_n, n_p and T and is independent of the interaction. The energies are not significantly altered by variations in K_s. Examining the three plots in fig. 7, the only appreciable variations occur either at supernuclear density or at high temperatures in the vicinity of the peak in the phase curves (compare fig. 6). This independence is largely due to the fact that electrons dominate the internal energy and pressure except at high densities and/or temperatures. Furthermore, at high temperatures and low densities, where nuclei are dissociated, the nucleons are effectively non-interacting and the value of K_s becomes irrelevant. At low density where the energies of nuclei are important, the density of matter in nuclei does not significantly differ from n_s, because of the relatively large values of K_s. Both $n_i - n_s$ and the compressional contribution to the energy are proportional to $1/K_s$ under these conditions.

To facilitate comparison of our results with those of CB, we examine the behavior of the EOS in the vicinity of the phase transition between nuclei and bulk matter for the $s = 1$ and $s = 1.5$ adiabats.

Fig. 8 displays the temperature along an isentrope of $s = 1$ with $Y_e = 0.3$ for the three incompressibilities, together with the results of LLPR ($K_s = 375$ MeV) and CB ($K_s = 180$ MeV). The difference between the $K_s = 375$ MeV and LLPR curves are

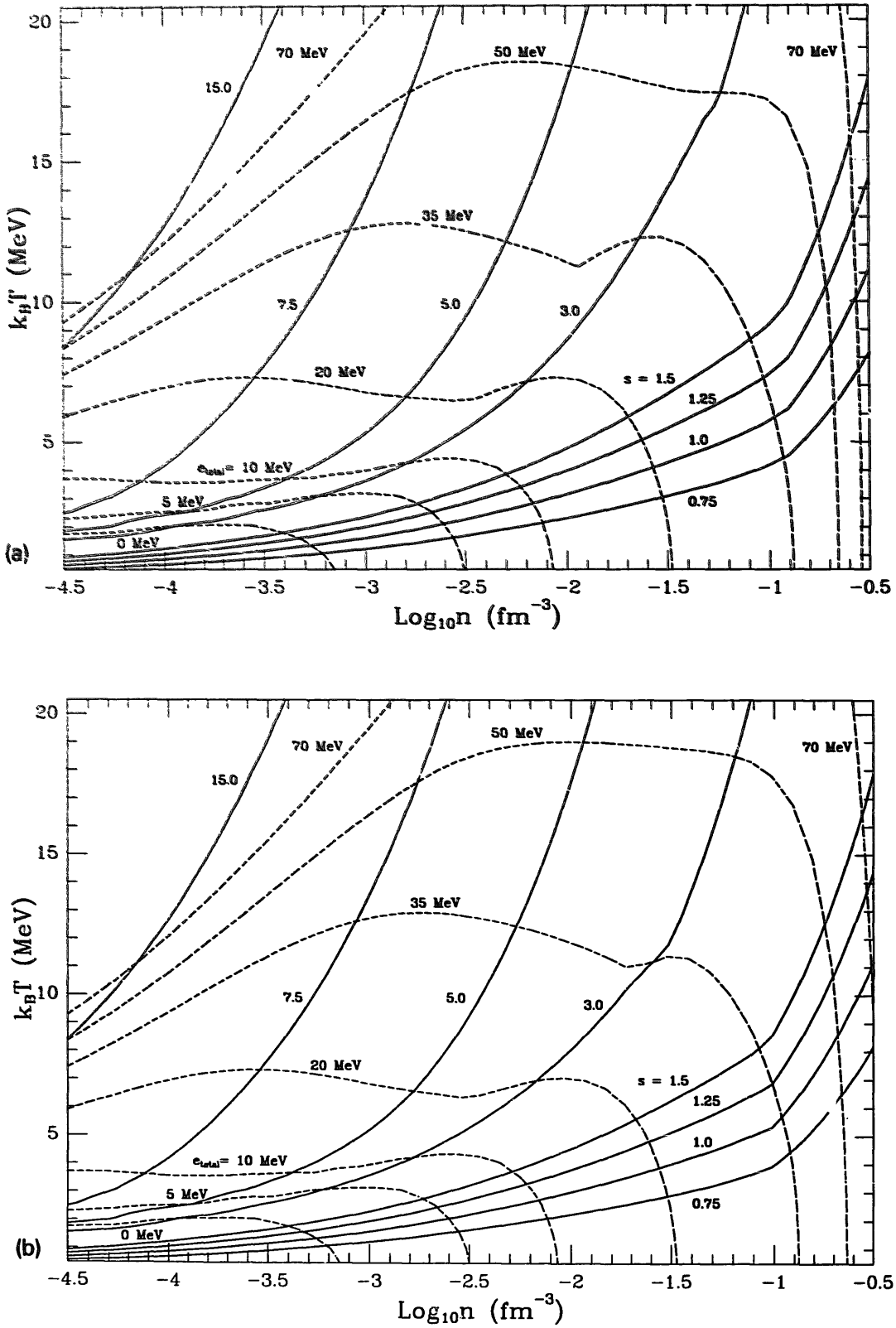

Fig. 7. Adiabats and isoergs for the case $Y_e = 0.3$ and for (a) $K_\nu = 375$ MeV, (b) $K_\nu = 220$ MeV and (c) $K_\nu = 180$ MeV. Solid lines denote adiabats, dashed lines denote isoergs.

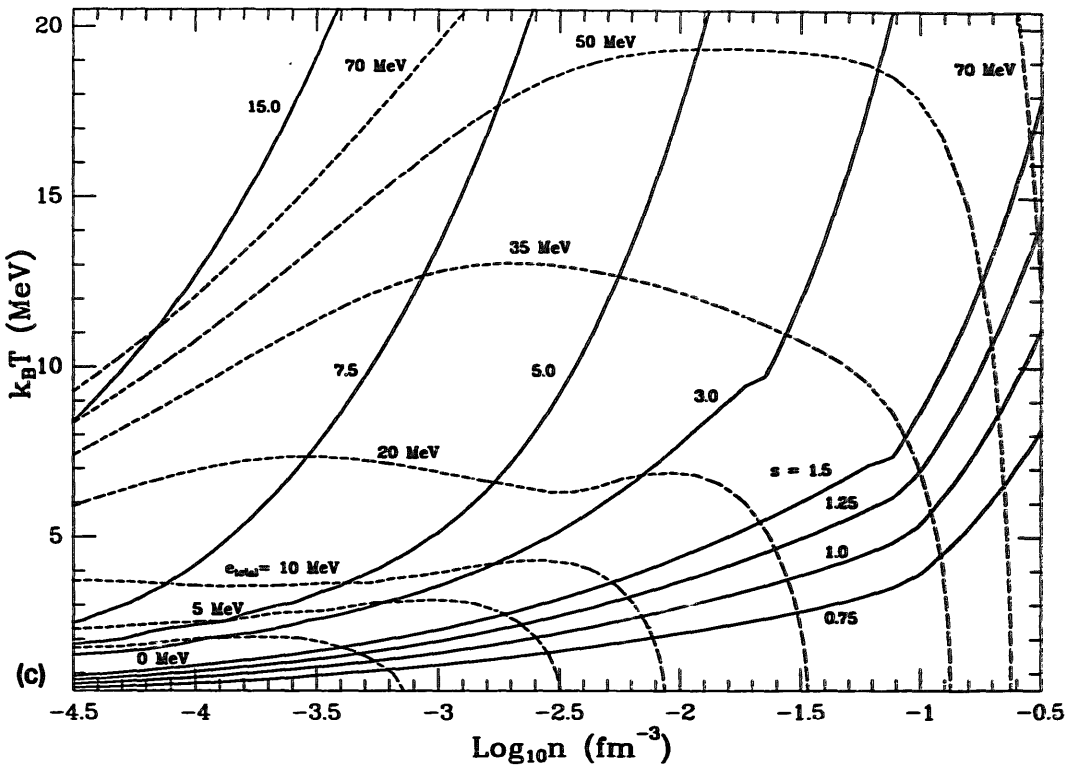

Fig. 7—continued.

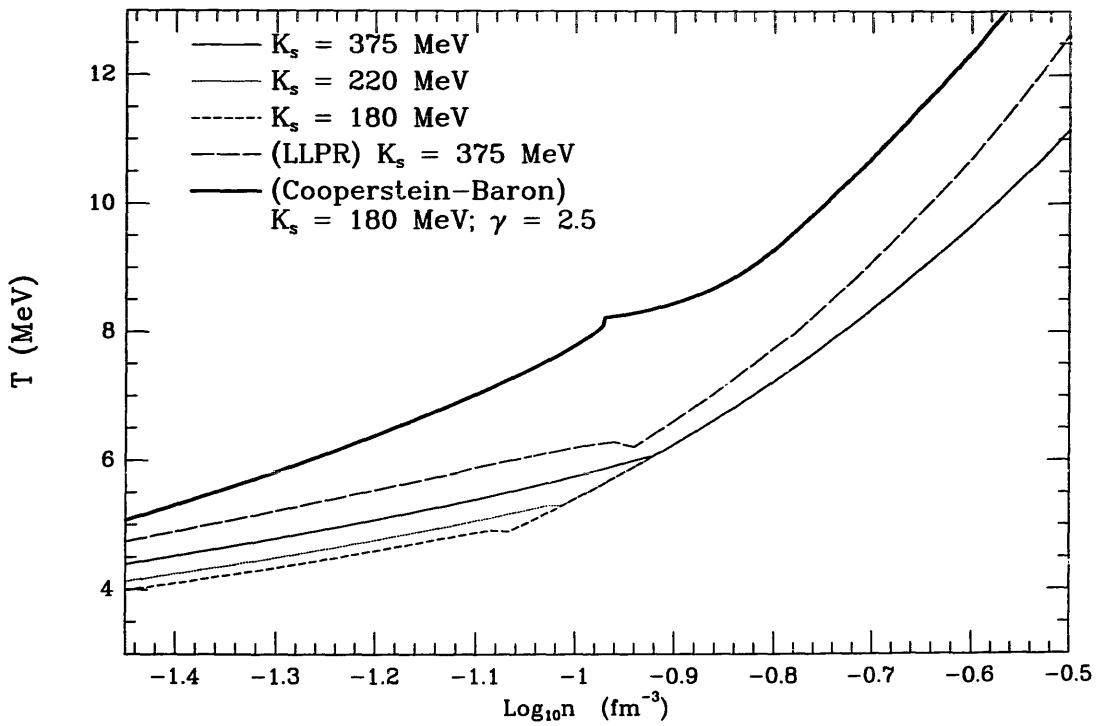

Fig. 8. Temperature in MeV along the $s = 1$ adiabat for the case $Y_e = 0.3$. Shown are cases taken from this work ($K_s = 375$, 220 and 180 MeV), from LLPR, and from CB.

due to the choice of effective mass. The difference between the $K_s = 180$ MeV and CB adiabats is due to CB's lower nuclear specific heat. Note also the increase in entropy at constant temperature, i.e., the slight drop in temperature at constant entropy, as one moves across the Maxwell construction, visible in LLPR's and our results. The CB EOS displays the opposite behavior, however. Finally, as discussed in reference to fig. 7, above the phase transition density, the temperature along adiabats becomes independent of K_s in our model.

Fig. 9 shows P/n along the same adiabats. All curves display a drop in P/n associated with the phase transition to bulk nuclear matter. Although it has been stated [43]) that this dip is unphysical, it is a natural consequence of the fact that the pressure is constant through the Maxwell construction region. In fact, the LLPR curve has two dips, since the additional transition between nuclei and bubbles exists in it. We again point out that the value of the pressure at densities below these transitions is largely independent of the bulk incompressibilities and the nuclear parameterizations and largely reflects the dominance of the electron pressure at these densities. The slight differences that are visible can be attributed to temperature effects. However, at supernuclear densities, both the value of K_s and the parameterization of the nucleon-nucleon force are important. The nearly constant difference between the $K_s = 375$ MeV and LLPR curves is due to the effective mass, and the difference between the $K_s = 180$ MeV and CB curves is due to functional form of the pressure-density relation. To obtain the supernuclear pressures that CB obtain we would have to employ $K_s \approx 60$ MeV.

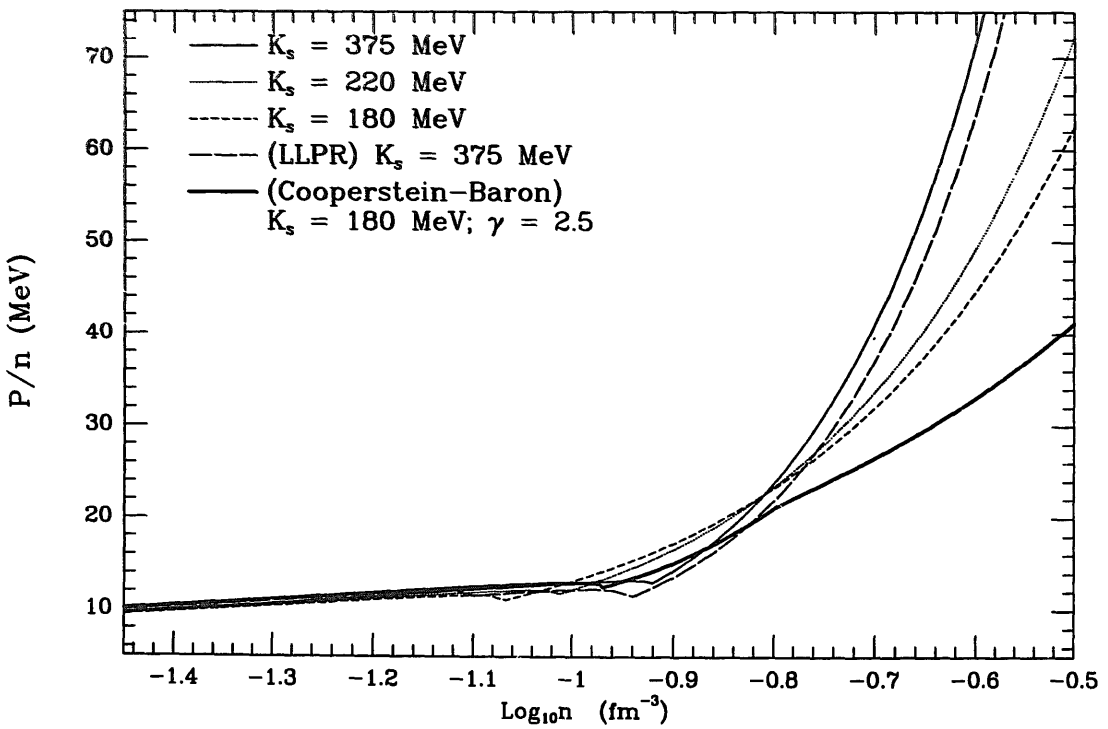

Fig. 9. Same as fig. 8, except for the pressure divided by baryon number density (in units of MeV).

The stiffening of the EOS as one goes from matter with nuclei to bulk matter is best shown by reference to the adiabatic index,

$$\Gamma = \left.\frac{\mathrm{d}\log P}{\mathrm{d}\log n}\right|_s, \tag{5.3}$$

which is shown in figs. 10 and 11 for $s=1$ and $s=1.5$, respectively, and $Y_e=0.3$. The transition is marked by a steep drop in Γ. The Maxwell construction softening forces Γ nearly to zero since the pressure along an adiabat through the coexistence region is almost constant. The adiabatic index does not drop completely to zero in this region since the temperature *and not the entropy* of both the nuclear and bulk phases must be the same. For this reason, the entropy actually increases slightly as one moves across the coexistence region at constant temperature[44]). This effect is more pronounced in fig. 11 for $s=1.5$ as can readily be seen. The LLPR EOS has two transitions as discussed previously. The transition to bulk matter occurs at densities very nearly the same as in the $K_s=375$ MeV case, and above and below this transition, the Γ's agree very well.

Note the trends that the Maxwell construction region becomes wider, and moves to lower density, with decreasing K_s. Both of these features may be understood as follows:

From eq. (3.6), the value of $u \approx n/n_s$ at the midpoint of the transition, where the energy of the uniform matter and nuclei phases are approximately equal, obviously decreases with decreasing K_s. In addition, the lower the value of u at the transition,

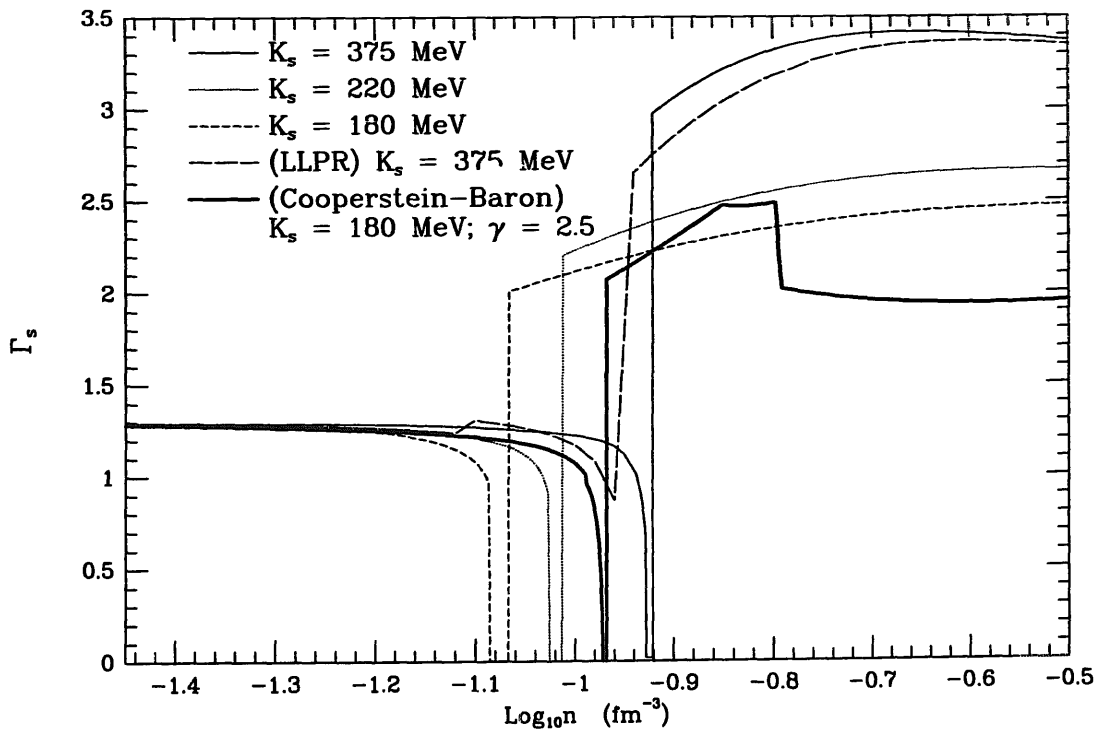

Fig. 10. Same as fig. 8, except for the adiabatic index Γ.

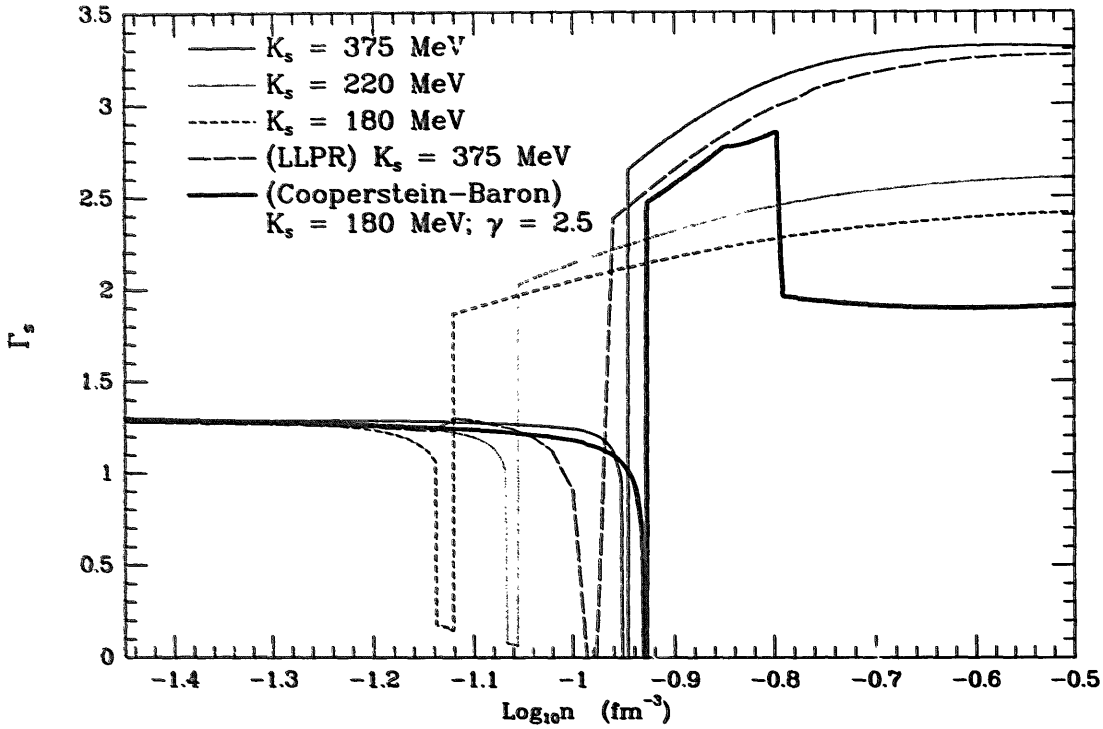

Fig. 11. Same as fig. 10, except that $s = 1.5$.

the larger is the energy change across the transition, and, thus, the larger is the width of the transition [44]). In comparison, the CB phase transition is rather narrow, occurs at a higher density than for the $K_s = 180$ MeV case, and moves up in density as the entropy is increased. Also note the relatively low value of Γ at supernuclear densities.

We have done preliminary testing of the EOS in some basic hydrodynamics codes. One particularly important test of the EOS [45,46]) is that of thermodynamic consistency in gravitational collapse. That is to say, in an adiabatic collapse the entropy should remain constant. In test collapses with a newtonian hydrodynamics code we have found that the entropy is conserved to better than one percent over the approximately one thousand timesteps that it took for our simulation to pass the "bounce" stage. Additionally, we have checked for internal consistency among the thermodynamic quantities such as free energy, pressure, etc. We have found no regions of the (n, T, Y_e) space where there are any substantial inconsistencies.

Although we have verified that the EOS code returns reasonable values throughout the entire relevant (n, T, Y_e) space, some minor discontinuities in pressure and energy may exist as one passes through the uppermost parts of the phase boundaries. These discontinuities are most pronounced for Y_e values less than 0.2, but are confined to temperatures near the peak in the phase boundaries and have relative magnitudes which are never more than ~1–2 percent. The existence of these discontinuities leads to the "bumps" in the upper portions of the phase boundaries observed in fig. 6. These discontinuities result from the inability of the Newton-

Raphson iteration scheme to converge for a limited set of conditions. When such a non-convergence takes place, the code return values for thermodynamic quantities by assuming uniform matter. The inability to converge results from inaccuracies in our parameterizations of the surface, translational and Coulomb energies, or from the existence of multiple solutions, which are most pronounced at high temperatures. Such conditions will not be encountered during the dynamical collapse and bounce phases of supernovae simulations. These conditions may be achieved, however, during the cooling of the protoneutron star within a few seconds after collapse [47]). Nevertheless, the protoneutron star is quasi-static and these small discontinuities are unlikely to present problems in hydrodynamic or hydrostatic simulations under such conditions. We have also restricted, in our code, input values of Y_e to the range 0.03–0.51 and T to values greater than 0.05 MeV. This is done only for convenience, and does not represent a limitation of the EOS. These conditions will never be encountered during supernovae simulations. Even in cold neutron stars, Y_e is in general larger than 0.04.

The EOS code is rapid enough to be used in a realistic hydrodynamical simulation and has been designed to allow easy incorporation into existing radiation hydrodynamics codes. The EOS code can be obtained by contacting the authors. Because the derivatives of thermodynamic quantities are analytically evaluated, this EOS code eliminates the need to numerically evaluate derivatives, thus requiring fewer calls to the EOS and further enhancing computational speed. We would like to point out one aspect of the EOS that allows for optimal computational efficiency. Typically, in hydrodynamical codes one solves the energy equation

$$e^{n+1} = e^n - \tfrac{1}{2}(P^{n+1} + P^n)\,dV \tag{5.4}$$

iteratively, adjusting the new internal energy, e^{n+1}, until the new value of the pressure, P^{n+1}, and e^{n+1} are consistent with eq. (5.4). Usually, the internal energy is taken as an independent variable in these codes. While we have written our EOS code to accommodate either the internal energy or temperature as inputs, the use of internal energy necessarily introduces another level of iteration in the EOS code. If one chooses to view both the energy and pressure as functions of temperature and then to iterate on temperature until the first law is satisfied, the computational effort is significantly reduced. In addition, as can be seen from fig. 7, at each density and Y_e there exists a minimum value for e. The use of e as an independent variable can be dangerous since transport or an iterative step may reach a value of e which is less than this minimum value. The choice of T as the independent variable obviates this problem.

6. Conclusions

The EOS described here is designed specifically to be rapid enough for use in radiation hydrodynamic codes, while still accurate in its modeling of the underlying

physics. It permits the consistent alteration of the major nuclear-force parameters, which is important given the current uncertainty in our knowledge of these parameters. The general formalism developed herein can easily be adjusted to allow more detailed nucleon-nucleon interactions, including those with finite-range forces, to be used. The model for nuclei is based upon the finite-temperature liquid-drop model, and includes the effects of translation, the Coulomb lattice, and the external nucleon vapor. Nucleon-nucleon interactions and degeneracy are included in the treatment of the external nucleons. The electron EOS is treated separately and treatments other than our own may be easily substituted. Comparison with the EOS of LLPR shows that, with the same set of nuclear parameters, reasonable agreement is obtained. We have discussed the major ways in which the EOS presented here differs from those of LLPR and CB. This code should eliminate the need for table construction and usage. It also supplies derivatives of the thermodynamic quantities with respect to density, temperature, and electron fraction, for use in hydrodynamics and transport codes. The use of this code should allow easier comparisons between simulations conducted with differing nuclear-force parameters, including the compression modulus and symmetry energies, and should illuminate the role of the EOS in the supernova problem.

We owe debts of gratitude to Adam Burrows and Amos Yahil, who have substantially contributed to earlier, preliminary versions of the equation of state presented in this paper. We also thank Jerry Cooperstein for the derivation of eq. (C.1), and both he and Edward Baron for discussions and for providing us with the Cooperstein-Baron EOS. Additionally, F.D.S. would like to thank Eric Myra and Noam Sack for the many hours of patient tutoring they have supplied. This research was supported in part by the US Dept. of Energy under grant No. DE-FG02-87ER40317.

Note added in proof: Since this paper was submitted, we have considered implementing a minor change to the EOS algorithm: the function h, defined in eq. (2.28), would have an overall exponent of 3 instead of 2. This ensures that $h'' = \partial^2 h/\partial x_i^2 \to 0$ and $\partial^2 h/\partial T^2 \to 0$ as $T \to T_c$, which is not the case with the present definition. This change eliminates the convergence problems that produce the "bumps" in the phase boundaries near T_c seen in fig. 6. Moreover, this change increases the nuclear surface specific heat contribution by 50%, which improves the overall agreement with the results of ref. [41]) and with nuclear systematics.

In addition, a version of the EOS that includes the liquid droplet form of the symmetry energy, i.e., includes the effects of a neutron skin, is being developed. As discussed in sect. 2.6, this change necessitates solving a five-dimensional Newton-Raphson iteration, compared to the three-dimensional scheme described herein. However, this change actually increases the speed of convergence near the phase boundaries, a result that was also pointed out to us by Jerry Cooperstein. We have not yet determined if the overall speed of the five-dimensional code is greater or

less than that of the three-dimensional code in hydrodynamic simulations, in which zones rarely pass through phase boundaries.

Appendix A

DERIVATIVE MATRIX FOR THE THREE-DIMENSIONAL SCHEME

In this appendix the derivatives of the three equilibrium conditions eq. (4.4) are written out. We use the information that the bulk properties of matter inside nuclei (P_i, μ_{ni} and μ_{pi}) are explicit functions of n_i and x_i alone, while those of matter outside nuclei (P_0+P_α, μ_{no} and μ_{po}) are explicit functions of n_{no} and n_{po} alone. The finite-size terms in the equilibrium equations (the B's) are explicit functions of n_i, x_i and u. Since n_α is an explicit function of μ_{no} and μ_{po}, we also have from eqs. (4.1) that x_i and u are explicit functions of n_i, n_{no} and n_{po}. It is convenient to write the three equilibrium conditions in the form (cf. eqs. (4.4) and (4.5))

$$A_k = A_{ki}(x_i, n_i) - B_k(x_i, n_i, u) - A_{ko}(n_{no}, n_{po}), \tag{A.1}$$

where subscripts i and o refer to the matter inside nuclei and to the matter outside nuclei, respectively, and the subscripts $k = 1$-3 refer to P, μ_n and μ_p, respectively. For example, $A_{1i} = P_i$ and $A_{1o} = P_o + P_\alpha$. We may therefore write

$$\frac{\partial A_{ki}}{\partial z_j} = \begin{cases} \left.\dfrac{\partial A_{ki}}{\partial n_i}\right|_{x_i} + \left.\dfrac{\partial A_{ki}}{\partial x_i}\right|_{n_i} \left.\dfrac{\partial x_i}{\partial n_i}\right|_{\eta_{no},\eta_{po}} & z_j = n_i \\ \left.\dfrac{\partial A_{ki}}{\partial x_i}\right|_{n_i} \left.\dfrac{\partial x_i}{\partial n_{no}}\right|_{n_i,n_{po}} & z_j = n_{no} \\ \left.\dfrac{\partial A_{ki}}{\partial x_i}\right|_{n_i} \left.\dfrac{\partial x_i}{\partial n_{po}}\right|_{n_i,n_{no}} & z_j = n_{po}\,. \end{cases} \tag{A.2}$$

Similarly,

$$\frac{\partial B_k}{\partial z_j} = \begin{cases} \left.\dfrac{\partial B_k}{\partial n_i}\right|_{x_i,u} + \left.\dfrac{\partial B_k}{\partial x_i}\right|_{n_i,u} \left.\dfrac{\partial x_i}{\partial n_i}\right|_{n_{no},n_{po}} + \left.\dfrac{\partial B_k}{\partial u}\right|_{n_i,x_i} \left.\dfrac{\partial u}{\partial n_i}\right|_{n_{no},n_{po}} & z_j = n_i \\ \left.\dfrac{\partial B_k}{\partial x_i}\right|_{n_i,u} \left.\dfrac{\partial x_i}{\partial n_{no}}\right|_{n_i,n_{po}} + \left.\dfrac{\partial B_k}{\partial u}\right|_{n_i,x_i} \left.\dfrac{\partial u}{\partial n_{no}}\right|_{n_i,n_{po}} & z_j = n_{no} \\ \left.\dfrac{\partial B_k}{\partial x_i}\right|_{n_i,u} \left.\dfrac{\partial x_i}{\partial n_{po}}\right|_{n_i,n_{no}} + \left.\dfrac{\partial B_k}{\partial u}\right|_{n_i,x_i} \left.\dfrac{\partial u}{\partial n_{po}}\right|_{n_i,n_{no}} & z_j = n_{po} \end{cases} \tag{A.3}$$

and

$$\frac{\partial A_{ko}}{\partial z_j} = \begin{cases} 0 & z_j = n_i \\ \left.\dfrac{\partial A_{ko}}{\partial n_{no}}\right|_{n_{po}} & z_j = n_{no} \\ \left.\dfrac{\partial A_{ko}}{\partial n_{po}}\right|_{n_{no}} & z_j = n_{po}\,. \end{cases} \tag{A.4}$$

The derivatives of B_k may be easily obtained from eqs. (4.5) and will not be given explicitly here. The derivatives of A_{ki} and A_{ko} are found by exploiting the thermo-

dynamic relationships for the chemical potentials and pressure of the bulk fluids. We will employ the notation for the isospin such that $t(-t) = \mathrm{n(p)}$ or p(n), and, in the following two equations, n_t refers to either n_{ti} or n_{to}, μ_t to μ_{ti} or μ_{to}, and P to P_i or P_o:

$$\left.\frac{\partial \mu_r}{\partial n_t}\right|_{n_{-t}} = \frac{TG_r}{n_r}\left[\delta_{tr} + \frac{3n_r m_r^*}{\hbar^2}(\alpha_2 + (\alpha_1 - \alpha_2)\delta_{tr})\right] + \left.\frac{\partial V_r}{\partial n_t}\right|_{n_{-t}}, \tag{A.5a}$$

$$\left.\frac{\partial P}{\partial n_t}\right|_{n_{-t}} = \sum_r n_r \left.\frac{\partial \mu_r}{\partial n_t}\right|_{n_{-t}}. \tag{A.5b}$$

Here we have used r as another isospin label, δ_{ij} is the Kronecker delta, and

$$G_t \equiv \frac{2F_{1/2}(\eta_t)}{F_{-1/2}(\eta_t)}. \tag{A.6}$$

For the particular potential given by eq. (2.13), we find

$$\left.\frac{\partial V_r}{\partial n_t}\right|_{n_{-t}} = \left.\frac{\partial(\alpha_1 \tau_r + \alpha_2 \tau_{-r})}{\partial n_t}\right|_{n_{-t}} + 2a + 4b\delta_{-tr} + \delta(1+\delta)c(n_n + n_p)^{\delta-1}, \tag{A.7}$$

where

$$\left.\frac{\partial \tau_r}{\partial n_t}\right|_{n_{-t}} = \frac{m_r^*}{\hbar^2}\left[3TG_r\delta_{tr} + \left(\frac{9m_r^*}{\hbar^2}Tn_rG_r - 5\tau_r\right)(\alpha_2 + (\alpha_1 - \alpha_2)\delta_{tr})\right]. \tag{A.8}$$

These equations may be used directly to find derivatives of μ_{no}, μ_{po} and P_o. Eq. (4.2) may be employed to find derivatives of P_α:

$$\left.\frac{\partial P_\alpha}{\partial n_{to}}\right|_{n_{-to}} = T\left.\frac{\partial n_\alpha}{\partial n_{to}}\right|_{n_{-to}} = n_\alpha \sum_r (2 - n_{ro}v_\alpha)\left.\frac{\partial \mu_{ro}}{\partial n_{to}}\right|_{n_{-to}}. \tag{A.9}$$

To get the proper derivatives for the inside bulk fluids, that is, ones taken with respect to n_i and x_i instead of n_{ni} and n_{pi}, one may make use of the following relations, combined with eqs. (A.5):

$$\left.\frac{\partial}{\partial n_i}\right|_{x_i} = (1 - x_i)\left.\frac{\partial}{\partial n_{ni}}\right|_{n_{pi}} + x_i \left.\frac{\partial}{\partial n_{pi}}\right|_{n_{ni}},$$

$$\left.\frac{\partial}{\partial x_i}\right|_{n_i} = n_i\left(\left.\frac{\partial}{\partial n_{pi}}\right|_{n_{ni}} - \left.\frac{\partial}{\partial n_{ni}}\right|_{n_{pi}}\right). \tag{A.10}$$

It is worth mentioning that if the form of the nuclear force used has $\alpha_1 = \alpha_2 = 0$, eqs. (A.5a) and (A.7) are simplified considerably.

The remaining derivatives to be evaluated are those of u and x_i, which, using eq. (4.1), are:

$$\left.\frac{\partial u}{\partial n_i}\right|_{n_{no},n_{po}} = -\frac{u}{n_1},$$

$$\left.\frac{\partial u}{\partial n_{to}}\right|_{n_i,n_{-to}} = -\frac{1-u}{n_1}\left[1-n_\alpha v_\alpha+(4-v_\alpha(n_{no}+n_{po}))\left.\frac{\partial n_\alpha}{\partial n_{to}}\right|_{n_{-to}}\right],$$

$$\left.\frac{\partial x_i}{\partial n_i}\right|_{n_{no},n_{po}} = \frac{(n_2-x_i n_1)}{n_i n_1},$$

$$\left.\frac{\partial x_i}{\partial n_{to}}\right|_{n_i,n_{-to}} = -\frac{n_2}{n_i u}\left.\frac{\partial u}{\partial n_{to}}\right|_{n_i,n_{-to}} - \frac{1-u}{n_i u}$$

$$\times\left[\delta_{tp}(1-n_\alpha v_\alpha)+(2-n_{po}v_\alpha)\left.\frac{\partial n_\alpha}{\partial n_{to}}\right|_{n_{-to}}\right]. \qquad \text{(A.11)}$$

In these expressions we have used the shorthand $n_1 = n_i-(n_{no}+n_{po})(1-n_\alpha v_\alpha)-4n_\alpha$ and $n_2 = n_i x_i - n_{po}(1-n_\alpha v_\alpha)-2n_\alpha$, and $\partial n_\alpha/\partial n_{to}$ is given in eq. (A.9).

Appendix B

DERIVATIVES OF THERMODYNAMIC QUANTITIES

In this appendix, derivatives of the "non-standard" variables P, e (internal energy per baryon) and s are obtained with respect to the "standard" variable set (n, Y_e, T). These quantities are useful if one wishes to call the equation of state with one or more "non-standard" variables. They are also necessary to calculate adiabatic indices.

We first consider only the baryon contributions, and use F, P, e and s to refer to only these contributions. The required derivatives are:

$$\frac{\partial P}{\partial n} = n\frac{\partial^2 F}{\partial n^2}, \qquad \frac{\partial P}{\partial Y_e} = n\left(\hat{\mu}_o+\frac{\partial^2 F}{\partial n\partial Y_e}\right), \qquad \frac{\partial P}{\partial T} = n\left(s+\frac{\partial^2 F}{\partial n\partial T}\right),$$

$$\frac{\partial s}{\partial n} = -\frac{1}{n^2}\frac{\partial P}{\partial T}, \qquad \frac{\partial s}{\partial Y_e} = -\frac{1}{n}\frac{\partial^2 F}{\partial T\partial Y_e}, \qquad \frac{\partial s}{\partial T} = -\frac{1}{n}\frac{\partial^2 F}{\partial T^2},$$

$$\frac{\partial e}{\partial n} = \frac{P}{n^2}+T\frac{\partial s}{\partial n}, \qquad \frac{\partial e}{\partial Y_e} = -\hat{\mu}_o+T\frac{\partial s}{\partial Y_e}, \qquad \frac{\partial e}{\partial T} = T\frac{\partial s}{\partial T}. \qquad \text{(B.1)}$$

We have used eq. (3.4), applied to baryons only, to obtain the above identities.

Straightforward manipulation yields the following expressions for the second derivatives of F:

$$\frac{\partial^2 F}{\partial n^2}=\frac{\partial \mu_n}{\partial n}-Y_e\frac{\partial \hat{\mu}}{\partial n}=\frac{\partial \mu_{no}}{\partial n}-Y_e\frac{\partial \hat{\mu}_o}{\partial n},$$

$$\frac{\partial^2 F}{\partial n \partial Y_e}=-\hat{\mu}-n\frac{\partial \hat{\mu}}{\partial n}=-\hat{\mu}_o-n\frac{\partial \hat{\mu}_o}{\partial n},$$

$$\frac{\partial^2 F}{\partial n \partial T}=\frac{\partial \mu_n}{\partial T}-Y_e\frac{\partial \hat{\mu}}{\partial T}=\frac{\partial \mu_{no}}{\partial T}-Y_e\frac{\partial \hat{\mu}_o}{\partial T},$$

$$\frac{\partial^2 F}{\partial Y_e \partial T}=-n\frac{\partial \hat{\mu}}{\partial T}=-n\frac{\partial \hat{\mu}_o}{\partial T},$$

$$\frac{\partial^2 F}{\partial T^2}=-n\frac{\partial s}{\partial T}. \tag{B.2}$$

We have used eqs. (3.4a) and (3.4b) in eq. (B.2). Thus, it is left only to evaluate $\partial\mu_{no}/\partial n$, $\partial\hat{\mu}_o/\partial n$, $\partial\mu_{no}/\partial T$, $\partial\hat{\mu}_o/\partial T$ and $\partial s/\partial T$. Such derivatives have to be evaluated with the recognition that the internal independent variables $z_j \equiv (n_i, n_{no}, n_{po})$ and the dependent variables $y_k \equiv (u, x_i)$ will change as $\lambda_i \equiv (n, T, Y_e)$ are each varied. The changes in z_j and y_k are constrained by the equilibrium conditions eqs. (4.4) and mass and charge conservation eqs. (3.1).

In general, therefore, derivatives of the quantities $\xi \equiv (\mu_{no}, \mu_{po}, T)$ may be written

$$\frac{\partial \xi}{\partial \lambda_i}=\left.\frac{\partial \xi}{\partial \lambda_i}\right|_{z,y}+\left.\frac{\partial \xi}{\partial z_j}\right|_{\lambda,y}\frac{\partial z_j}{\partial \lambda_i}+\left.\frac{\partial \xi}{\partial y_k}\right|_{\lambda,z}\left(\left.\frac{\partial y_k}{\partial \lambda_i}\right|_{z}+\left.\frac{\partial y_k}{\partial z_j}\right|_{\lambda}\frac{\partial z_j}{\partial \lambda_i}\right), \tag{B.3}$$

where we use the convention of implied summation over repeated indices. The changes in z with respect to those in λ are determined from eq. (4.4):

$$0=\left.\frac{\partial A_m}{\partial \lambda_i}\right|_{z,y}+\left.\frac{\partial A_m}{\partial z_j}\right|_{\lambda,y}\frac{\partial z_j}{\partial \lambda_i}+\left.\frac{\partial A_m}{\partial y_k}\right|_{\lambda,z}\left(\left.\frac{\partial y_k}{\partial \lambda_i}\right|_{z}+\left.\frac{\partial y_k}{\partial z_j}\right|_{\lambda}\frac{\partial z_j}{\partial \lambda_i}\right), \tag{B.4}$$

which may be inverted to yield

$$\left.\frac{\partial z_j}{\partial \lambda_i}\right|_{y}=-\left(\left.\frac{\partial A_m}{\partial z_j}\right|_{\lambda,y}+\left.\frac{\partial A_m}{\partial y_k}\right|_{\lambda,z}\left.\frac{\partial y_k}{\partial z_j}\right|_{\lambda}\right)^{-1}$$
$$\times\left(\left.\frac{\partial A_m}{\partial \lambda_i}\right|_{z,y}+\left.\frac{\partial A_m}{\partial y_k}\right|_{\lambda,z}\frac{\partial y_k}{\partial \lambda_i}\right). \tag{B.5}$$

The changes in y with respect to z are easily obtained from eqs. (A.11) and the

changes with respect to λ may be found from eqs. (4.1):

$$\frac{\partial u}{\partial n}=\frac{1}{n_1},$$

$$\frac{\partial u}{\partial T}=\frac{(1-u)[4-v_\alpha(n_{no}+n_{po})]}{n_1}\frac{\partial n_\alpha}{\partial T},$$

$$\frac{\partial x_i}{\partial n}=\frac{n_1 Y_e-n_2}{un_i n_1},$$

$$\frac{\partial x_i}{\partial T}=\frac{(n_i x_i-nY_e)[4-(n_{no}+n_{po})]+(n-n_i)(2-n_{po}v_\alpha)}{un_i n_1}\frac{\partial n_\alpha}{\partial T}, \tag{B.6}$$

where n_1 and n_2 are defined as in appendix A. Here, we must employ the relation

$$\frac{\partial n_\alpha}{\partial T}=\frac{n_\alpha}{T}\left(\tfrac{3}{2}-\mu_\alpha/T+\frac{\partial \mu_\alpha}{\partial T}\right). \tag{B.7}$$

The derivatives of the bulk variables (P, μ_n, μ_p) and the finite-size terms with respect to z and y are evaluated in appendix A, so the calculations of $(\partial A_m/\partial z)|_{\lambda,y}$ and $(\partial A_m/\partial_y)|_{\lambda,z}$ have already been done. The quantities $(\partial A_m/\partial n)|_{z,y}$ are trivially zero, since there is no explicit density dependence. The quantities $(\partial A_m/\partial T)|_{z,y}$ may be found with the assistance of the following, applied to bulk matter inside or outside nuclei:

$$\frac{\partial P}{\partial T}=n\left[s+\sum_t n_t\left.\frac{\partial \mu_t}{\partial T}\right|_{n_n,n_p}\right],$$

$$\left.\frac{\partial \mu_t}{\partial T}\right|_{n_n,n_p}=\left.\frac{\partial(T\eta_t+V_t)}{\partial T}\right|_{n_n,n_p}=\eta_t-\tfrac{3}{2}G_t+\sum_s\left(\frac{5\tau_s}{2T}-\frac{9m_s^*}{2\hbar^2}n_s G_s\right)(\alpha_2+(\alpha_1-\alpha_2)\delta_{ts}). \tag{B.8}$$

The derivatives $(\partial B_m/\partial T)$ are easily found from eqs. (4.5) and are not given here.

The last required derivative may be found by directly differentiating eq. (3.4c):

$$\begin{aligned}n\left.\frac{\partial s}{\partial T}\right|_{z,y}=&un_i\frac{\partial s_i}{\partial T}+(1-u)(1-n_\alpha v_\alpha)n_o\frac{\partial s_o}{\partial T}+(1-u)\frac{3n_\alpha}{2T}\\&+\frac{\beta\mathscr{D}}{9h^2}\left(\frac{\partial h}{\partial T}-4h\frac{\partial^2 h}{\partial T^2}\right)\\&+\frac{u(1-u)n_i}{A_o}\left[\frac{3h}{2T}+\left(5-2\frac{\mu_H}{T}\right)\frac{\partial h}{\partial T}-(\mu_H-T)\frac{\partial^2 h}{\partial T^2}\right].\end{aligned} \tag{B.9}$$

It is useful to note in this regard that entropy derivatives for the bulk fluids may be obtained from eqs. (2.16):

$$n\frac{\partial s}{\partial T}=\frac{1}{4T}\sum_t\left(\frac{5\hbar^2\tau_t}{m_t^*T}-9n_t G_t\right). \tag{B.10}$$

In this expression, n, s, m^* and τ refer to the bulk matter quantities inside or outside the nucleus.

The full derivatives eqs. (B.1) are found by combining the results for the baryons with those for the electrons and the photons, which are given in appendix C.

Appendix C

LEPTON AND PHOTON ENERGIES

For the purposes of this paper, it is sufficient to assume that leptons (electrons and neutrinos) are relativistic, and that the temperature is high enough to ensure particle-antiparticle pair equilibrium. Letting m_l be the rest mass of the lepton to be considered, one can show that keeping the lowest order mass corrections in the extremely relativistic limit, for any degree of degeneracy, results in

$$nY_l = \frac{g_l}{6\pi^2}\left(\frac{\mu_l}{\hbar c}\right)^3 [1+\mu_l^{-2}(\pi^2T^2-\tfrac{3}{2}m_l^2c^4)], \tag{C.1}$$

where Y_l is the net number of the particular lepton per baryon (i.e., the number of particles minus the number of antiparticles), g_l is the spin degeneracy and μ_l is the lepton's chemical potential. The chemical potential may be found from solving eq. (C.1), which is a cubic:

$$\mu_l = r - q/r, \qquad r = [\sqrt{q^3+t^2}+t]^{1/3}, \tag{C.2}$$

where $t = 3\pi^2(\hbar c)^3 nY_l/g_l$ and $q = \frac{1}{3}(\pi T)^2 - \frac{1}{2}m_l^2c^4$. Expressions for the pressure and entropy per baryon are:

$$P_l = \frac{g_l\mu_l}{24\pi^2}\left(\frac{\mu_l}{\hbar c}\right)^3\left[1+\mu_l^{-2}(2\pi^2T^2-3m_l^2c^4)+\frac{\pi^2T^2}{\mu_l^4}(\tfrac{7}{15}\pi^2T^2-\tfrac{1}{2}m_l^2c^4)\right],$$

$$s_l = \frac{g_lT\mu_l^2}{6n(\hbar c)^3}[1+\mu_l^{-2}(\tfrac{7}{15}\pi^2T^2-\tfrac{1}{2}m_l^2c^4)].$$

$$e_l = \frac{g_l\mu_l}{8\pi^2 n}\left(\frac{\mu_l}{\hbar c}\right)^3\left[1+\mu_l^{-2}(2\pi^2T^2-m_l^2c^4)+\frac{\pi^2T^2}{\mu_l^4}(\tfrac{7}{15}\pi^2T^2-\tfrac{1}{2}m_l^2c^4)\right]. \tag{C.3}$$

For completeness, we also write down the expressions for a photon gas ($\mu_\gamma = 0$):

$$P_\gamma = \frac{\pi^2T^4}{45(\hbar c)^3}, \qquad s_\gamma = \frac{4P_\gamma}{nT}, \qquad e_\gamma = \frac{3P_\gamma}{n}. \tag{C.4}$$

The approximation eq. (C.1) for electrons will break down at densities below 10^9 g · cm^{-3} and temperatures below 1 MeV, and in this regime, explicit solution of the appropriate Fermi integrals is necessary [cf. Cooperstein *et al.* [12])]. However, the lepton and photon energies are independent of the baryonic equation of state and the use of a different algorithm for these energies will leave the baryonic EOS unaltered.

Finally, for reference, we include the derivatives for electrons (using $g_e = 2$):

$$\frac{\partial P_e}{\partial n} = \frac{Y_e}{n}\frac{\partial P_e}{\partial Y_e} = nY_e\frac{\partial \mu_e}{\partial n} = \frac{\pi^2 n Y_e^2 (\hbar c)^3}{\mu_e^2 + \frac{1}{3}\pi^2 T^2 - \frac{1}{2}m_e^2 c^4},$$

$$\frac{\partial P_e}{\partial T} = n\left(s_e + Y_e\frac{\partial \mu_e}{\partial T}\right) = n\left(s_e - \frac{2\mu_e T}{3(\hbar c)^3}\frac{\partial \mu_e}{\partial n}\right),$$

$$\frac{\partial n s_e}{\partial n} = Y_e\frac{\partial s_e}{\partial Y_e} = s_e - \frac{1}{n}\frac{\partial P_e}{\partial T},$$

$$\frac{\partial s_e}{\partial T} = \frac{s_e}{T} + \frac{2}{3n(\hbar c)^3}\left(\tfrac{7}{15}\pi^2 T^2 + \mu_e T\frac{\partial \mu_e}{\partial T}\right),$$

$$\frac{\partial n e_e}{\partial n} = Y_e\frac{\partial e_e}{\partial Y_e} = Y_e\left(\mu_e - T\frac{\partial \mu_e}{\partial T}\right),$$

$$\frac{\partial e_e}{\partial T} = T\frac{\partial s_e}{\partial T}. \tag{C.5}$$

The photon derivatives are easily found to be:

$$\frac{\partial P_\gamma}{\partial n} = 0, \qquad \frac{\partial P_\gamma}{\partial T} = n s_\gamma,$$

$$\frac{\partial s_\gamma}{\partial n} = s_\gamma / n, \qquad \frac{\partial s_\gamma}{\partial T} = 3 s_\gamma / T,$$

$$\frac{\partial e_\gamma}{\partial n} = -\tfrac{3}{4} T s_\gamma / n, \qquad \frac{\partial e_\gamma}{\partial T} = 3 s_\gamma. \tag{C.6}$$

All derivatives of photon quantities with respect to Y_e are zero.

References

1) M.F. El Eid and W. Hillebrandt, Astron. Astrophys. Suppl. Ser. **42** (1980) 215
2) T.J. Mazurek, J.M. Lattimer and G.E. Brown, Ap. J. **229** (1979) 713
3) J.W. Negele and D. Vautherin, Nucl. Phys. **A207** (1973) 298
4) P. Bonche and D. Vautherin, Nucl. Phys. **A372** (1981) 496
5) R.G. Wolff, thesis, Technische Universität, München (1983)
6) S. Marcos, M. Barranco and J.-R. Buchler, Nucl. Phys. **A389** (1982) 507
7) R. Ogasawara and K. Sato, Prog. Theor. Phys. **70** (1983) 1569
8) E. Suraud, in Problems of collapse and numerical relativity, ed. D. Bancel and M Signore (Reidel, Dordrecht, 1984) p. 81
9) J.M. Lattimer, C.J. Pethick, D.G. Ravenhall and D.Q. Lamb, Nucl. Phys. **A432** (1985) 646
10) J.M. Lattimer, unpublished
11) K.A. van Riper, in Supernova remnants and their X-ray emission, ed. J. Danziger and P. Gorenstein (Reidel Dordrecht, 1983) p. 471; Ap. J. Suppl. **75** (1991) 449
12) J. Cooperstein, Nucl. Phys. **A429** (1985) 527
13) J. Cooperstein and E.A. Baron, in Supernovae, ed. A. Petschek (Springer, New York, 1990)
14) A. Burrows and J.M. Lattimer, Ap. J. **307** (1986) 178

15) S. Bruenn, Ap. J. **341** (1989) 385
16) E. Myra and S. Bludman, Ap. J. **340** (1989) 384
17) A. Burrows and J.M. Lattimer, Ap. J. **285** (1984) 294
18) G. Baym, H.A. Bethe and C.J. Pethick, Nucl. Phys. **A175** (1971) 225
19) D.Q. Lamb, J.M. Lattimer, C.J. Pethick and D.G. Ravenhall, Phys. Rev. Lett. **41** (1978) 1623
20) D.G. Ravenhall, C.J. Pethick and J.R. Wilson, Phys. Rev. Lett. **150** (1985) 2006
21) W.D. Myers and W.J. Swiatecki, Ann. of Phys. **84** (1973) 186
22) J.M. Pearson, Y. Aboussir, A.K. Dutta, R.C. Nayak, M. Farine and F. Tondeur, Nucl. Phys. **A528** (1991) 1
23) G.E. Brown and E. Osnes, Phys. Lett. **B154** (1985) 223
24) J.P. Blaizot, Phys. Reports **64** (1980) 171
25) M. M. Sharma, W.T.A. Borghols, S. Brandenburg, S. Crona, A. van der Woude and M. N. Harakeh, Phys. Rev. **C38** (1988) 2562
26) P. Gleissl, M. Brack, J. Meyer and P. Quentin, Ann. of Phys. **197** (1990) 205
27) J.M. Lattimer and D.G. Ravenhall, Ap. J. **223** (1978) 314
28) P. Möller and J.R. Nix, At. Data Nucl. Data Tables **39** (1988) 219
29) P. Möller, W.D. Myers, W.J. Swiatecki and J. Treiner, At. Data Nucl. Data Tables **39** (1988) 225
30) W.D. Myers, W.J. Swiatecki, T. Kodama, L.J. El-Jaick and E.R. Hilf, Phys. Rev. **C15** (1977) 2032
31) Vautherin and Brink, Phys. Rev. **C5** (1972) 626
32) F. Tondeur, M. Brack, M. Farine and J.M. Pearson, Nucl. Phys. **A420** (1984) 297
33) F. Tondeur, Nucl. Phys. **A442** (1985) 460
34) M. Barranco and J. Treiner, Nucl. Phys. **A351** (1981) 269
35) J.M. Lattimer, in The structure and evolution of neutron stars, ed. T. Tamagaki and S. Tsuruta (Addison-Wesley, New York, 1991)
36) M. Prakash, T.A. Ainsworth and J.M. Lattimer, Phys. Rev. Lett. **61** (1988) 2518
37) C. Gale, G.F. Bertsch and S. Das Gupta, Phys. Rev. **C35** (1987) 1666
38) D. Gogny, in Nuclear self-consistent fields, ed. G. Ripka and M. Porneuf (North-Holland, Amsterdam, 1975) p. 333
39) G.M. Walke, M. Prakash, T.T.S. Kuo, S. Das Gupta and C. Gale, Phys. Rev. **C38** (1988) 2101
40) K. Kolehmainen, M. Prakash, J.M. Lattimer and J.R. Treiner, Nucl. Phys. **A439** (1985) 535
41) D.G. Ravenhall, C.J. Pethick and J.M. Lattimer, Nucl. Phys. **A407** (1983) 571
42) J. Kapusta, Phys. Rev. **C29** (1984) 1735
43) H.A. Bethe, G.E. Brown, J. Cooperstein and J. R. Wilson, Nucl. Phys. **A403** (1983) 625
44) C.J. Pethick, D.G. Ravenhall and J.M. Lattimer, Nucl. Phys. **A414** (1984) 517
45) J. Cooperstein, PhD Thesis, State University of New York at Stony Brook (1982)
46) S. Bruenn, Ap. J. Suppl. **58** (1985) 771
47) A. Burrows and J.M. Lattimer, Ap. J. **307** (1986) 178
48) E. Baron, H.A. Bethe, G.E. Brown, J. Cooperstein and S. Kahana, Phys. Rev. Lett. **59** (1987) 736